arXiv:1703.00649v1 [cond-mat.mtrl-sci] 2 Mar 2017

Structural deformations of two-dimensional planar structures under uniaxial strain: The case of graphene

Zacharias G. Fthenakis
Institute of Electronic Structure and Laser, FORTH, Heraklion, Greece

Nektarios N. Lathiotakis
Theoretical and Physical Chemistry Institute, National Hellenic Research Foundation, Vass. Constantinou 48, GR-11635 Athens, Greece

(Dated: March 3, 2017)

In the present work, a method for the study of the structural deformations of two dimensional planar structures under uniaxial strain is presented. The method is based on molecular mechanics using the original stick and spiral model and a modified one which includes second nearest neighbor interactions for bond stretching. As we show, the method allows an accurate prediction of the structural deformations of any two dimensional planar structure as a function of strain, along any strain direction in the elastic regime, if structural deformations are known along specific strain directions, which are used to calculate the stick and spiral model parameters. Our method can be generalized including other strain conditions and not only uniaxial strain. We apply this method to graphene and we test its validity, using results obtained from *ab initio* Density Functional Theory calculations. What we find is that the original stick and spiral model is not appropriate to describe accurately the structural deformations of graphene in the elastic regime. However, the introduction of second nearest neighbor interactions provides a very accurate description.

PACS numbers: 61.48.Gh, 62.20.-x, 62.20.de, 62.20.dj, 62.20.dq, 62.20.F-, 62.23.Kn, 62.25.-g

I. INTRODUCTION

Undoubtedly, graphene is one of the most studied materials in recent years. This is due to its exotic properties, like for instance its high carrier mobility[1] and high thermal conductivity[2–4] at room temperature, its high strength[5,6], etc, which makes graphene one of the most interesting materials for future nanoelectronic and nanomechanic applications. Following graphene, several two dimensional (2D) materials have also gained interest, exhibiting interesting mechanical[7–14] and electronic properties. The world of 2D materials that have been brought to the center of attention recently[15,16] includes several transition metal dichalcogenides[10,17], (like for instance MoS_2 or WS_2), hexagonal BN (h-BN)[8,9,18,19], Si_2BN[14,20], Si_nB_m[21–23], SiX and XSi_3 (X=B, C, N, Al, P)[24], CdS[25], AlN[19,26–28], SiC, InN and GaN[19], C_2F[9], Silicene[11,12,29,30], Germanene[30], Siligene (SiGe)[31], Phosphorene[13,32], as well as several graphene allotropes, like pentaheptites and octagraphene[5,33], or other Carbon 2D allotropes, like pentagraphene[34], graphyne, graphydine[33,35], or graphene-based derivatives, like graphane and graphone[35,36] etc.

A special class of these materials are those which are entirely planar, like for instance several graphene allotropes (pentaheptites, octagraphene, etc)[5,33,37], as well as h-BN[18], Si_2BN[14,20], AlN, SiC, Si_nB_m[21–23], CdS[25], XSi_3 with X=B,C,Al[24] etc. In this work, we present a method for the study of the mechanical response, of these materials, e.g. bond stretching and angle bending deformations, in the presence of uniaxial tensile strain, providing analytic expressions for these deformations along any strain direction. Our method can be generalized including any other strain condition (i.e. not only uniaxial strain) and is based on molecular mechanics assuming two different versions of the so called *stick and spiral model*[38], which has been employed previously for the study of the mechanical properties of Carbon nanotubes[39–44].

As an example, we apply our method to graphene, providing analytic expressions for bond length and bond angle deformations under tensile strain. We test the accuracy of these expressions using results we obtain from ab-initio density functional theory (DFT) calculations. In particular, we calculate the structural deformations of graphene under tensile strain along the high symmetry arm chair and zig-zag directions, as well as two other randomly selected directions, which are perpendicular to each other. According to our findings, the original stick and spiral model is not sufficient to provide an accurate description of the mechanical deformations of graphene under tensile strain in the elastic regime, since the DFT results can not be reproduced accurately by the analytic expressions provided by that model. However, due to the coupling between the bond stretching and angle bending terms, which is inherently included in the modified stick and spiral model, this modified model provides a quite accurate description. Moreover, fitting these analytic expressions to the DFT results we calculate the force constants for bond stretching and angle bond bending for graphene, thus allowing the prediction of the mechanical response of graphene in the elastic regime for strain on any direction.

II. THE DEFORMATION ENERGY

In molecular mechanics approach the deformation energy U is a sum of energy contributions from different deformation modes[38]. In particular, U is written as

$$U = U_s + U_b + U_\omega + U_\tau + U_{vdw} + U_e, \quad (1)$$

where U_s, U_b, U_ω, U_τ, U_{vdw} and U_e correspond to the energy contributions from bond stretching, bond angle bending, bond inversion, bond angle torsion, Van der Walls interactions and electrostatic interactions, respectively. Since tensile strain in a 2D planar structure is in-plane strain, the terms U_ω and U_τ vanish. Moreover, since there are no interactions between different sheets of those 2D structures, the terms U_{vdw} and U_e also vanish. Thus, the deformation energy becomes

$$U = U_s + U_b. \quad (2)$$

U_s and U_b may be expressed in several different ways (see for instance Refs. 45–47). However, the simplest way is to be expressed as a sum of harmonic terms constituting the so-called *stick and spiral model*.

According to the stick and spiral model, the deformation energy per unit cell is written as a sum of energy contributions from each bond length and bond angle deformation. Each of these contributions has a quadratic dependence on the corresponding deformation, i.e. it is either of the form $(1/2)k_s\delta l^2$ (for bond stretching), or $(1/2)k_b\delta\phi_{ij}^2$ (for bond-angle bending), where k_s and k_b are the corresponding force constants, and δl and $\delta\phi$ the bond length and bond-angle deformations for each specific bond and bond angle, respectively. Thus, the deformation energy per unit cell is

$$U = \frac{1}{2}\sum_i \left(k_{s,i}\delta l_i^2 + \frac{1}{2}\sum_j k_{b,ij}\delta\phi_{ij}^2 \right), \quad (3)$$

where i counts all the bonds inside the unit cell and j counts the bonds which form bond angles with bond i. The $1/2$ factor of the second sum is to avoid double counting of the bonds.

In the description provided by the stick and spiral model, bond stretching and bond angle bending are not coupled. The energy provided by Eq. (3) does not have any terms mixing these deformations. In addition, as we will see later, in the minimization of the deformation energy under constant strain these deformations remain decoupled. More specifically, one arrives at two independent systems of analytic equations one for stretching and one for bending. A more accurate description would include a coupling term between these deformations. This can be achieved by introducing extra terms describing the stretching of second nearest neighbor interatomic distances. In the present work, we study both cases.

For a planar structure with three-fold coordinated atoms, there are three bonds and three bond angles per atom (see Fig. 1(a)). If we label i, j_1 and j_2 the bonds of atom A and i, j_3 and j_4 those of atom B, (the two atoms share the bond i), then the index j of Eq. (3) takes the values j_1, j_2, j_3 and j_4. Moreover, since the structure is planar, and all atoms remain in the plane under tensile strain

$$\phi_{ij_1} + \phi_{ij_2} + \phi_{j_1j_2} = \phi_{ij_3} + \phi_{ij_4} + \phi_{j_3j_4} = 2\pi, \quad (4)$$

where ϕ_{ij_1}, ϕ_{ij_2}, $\phi_{j_1j_2}$ are the bond angles of atom A and ϕ_{ij_3}, ϕ_{ij_4}, $\phi_{j_3j_4}$ the bond angles of atom B. Consequently,

$$\delta\phi_{ij_1} + \delta\phi_{ij_2} + \delta\phi_{j_1j_2} = \delta\phi_{ij_3} + \delta\phi_{ij_4} + \delta\phi_{j_3j_4} = 0. \quad (5)$$

In the present work we study structures with only 3-fold coordinated atoms, since this is the most common case. However, the generalization of our method to structures with n-fold coordinated atoms, with $n \neq 3$, is obvious.

Due to symmetry reasons (if any), several bonds length deformations (as well as bond angle deformations) may be equivalent with each other under specific strain conditions. In that case, U can be written as a function of only the independent bond length and bond angle deformations per unit cell, and Eq. (3) can be rewritten as

$$U = \frac{1}{2}\left(\sum_i n_i k_{s,i}\delta l_i^2 + \frac{1}{2}\sum_i\sum_j m_{ij}k_{b,ij}\delta\phi_{ij}^2 \right), \quad (6)$$

where n_i is the number of equivalent bond length deformations of type i and m_{ij} the number of equivalent bond angle deformations formed by the bonds which have independent bond length deformations of type i and j. i runs over the independent bond deformations only.

Under uniaxial strain, the deformation energy and the corresponding deformations δl_i and $\delta\phi_{ij}$ at the strained equilibrium can be found from the minimization of the deformation energy subject to constrains describing the strain condition. These constraints can be incorporated using the Lagrange multipliers technique. For constant uniaxial tensile strain ε there is only one constraint described by $\varepsilon = \delta L/L_0$, where L_0 is a length along the strain direction and δL the elongation of L_0 upon that strain, which should be expressed as a function of the independent variables δl_i and $\delta\phi_{ij}$. Thus, the function which should be minimized becomes

$$\Lambda = U + \lambda(\varepsilon - \delta L/L_0), \quad (7)$$

with λ the corresponding Lagrange multiplier. Obviously, for different strain conditions, different constrains will apply, which can be incorporated in Eq. (7) using the corresponding Lagrange multipliers. Thus, our method can be easily generalized to describe the structural deformations of a 2D planar structure, not only under uniaxial strain, but under any strain condition.

In order to minimize Λ in Eq. (7), with respect to the bond stretching and angle bending deformations, one needs to express δL in terms of these deformations.

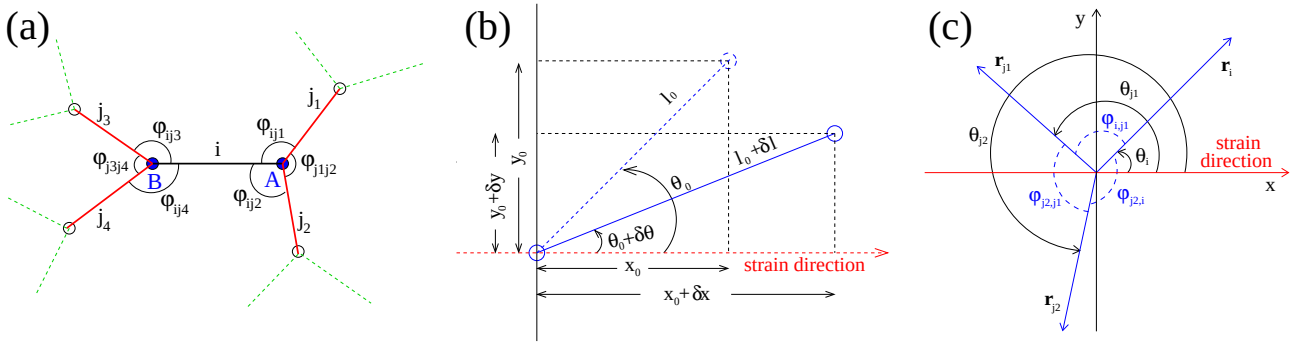

FIG. 1: (Color online) (a) Bond i of atoms A and B. Atom A forms the bonds i, j1 and j2 with its neighboring atoms and atom B forms the bonds i, j3 and j4, (b) Bond and angle deformations under uniaxial strain, (c) Relation between θ_i and ϕ_{ij}.

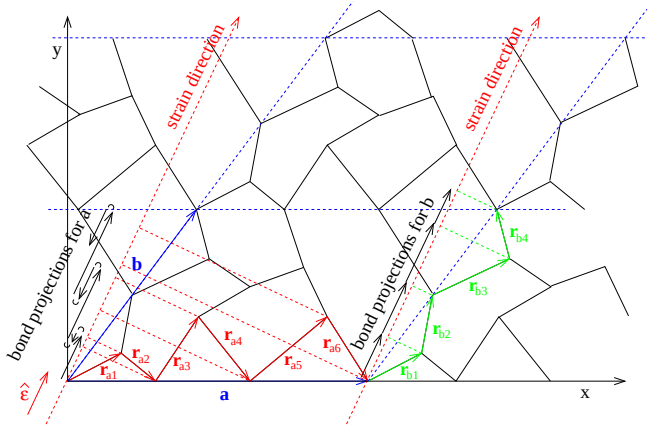

FIG. 2: (Color online) Periodic planar structure with 3-fold coordinated atoms strained along the strain direction $\hat{\boldsymbol{\varepsilon}}$ (colored in red). The unit cell vectors (colored in blue) are $\mathbf{a}$ and $\mathbf{b}$. The vector sum of the vectors $\mathbf{r}_{ai}$ ($\mathbf{r}_{bi}$) corresponding to the red (green) colored bonds, constitute the unit cell vector $\mathbf{a}$ ($\mathbf{b}$). The projection of those bond vectors along the strain direction are shown with black arrows along the strain direction.

A. δL as a function of bond deformations

Without loss of generality, we may assume that the structure is periodic. A non-periodic (i.e. amorphous) structure could be considered as periodic with infinite periodicity. For convenience, let us assume that the unit cell vectors for $\varepsilon = 0$ are $\mathbf{a}_0 = a_0\hat{\mathbf{i}}$ and $\mathbf{b}_0 = b_{x0}\hat{\mathbf{i}} + b_{y0}\hat{\mathbf{j}}$, as shown in Fig. 2. Let us apply tensile strain by stretching the structure along the line connecting two equivalent atoms in different unit cells. The vector connecting those two atoms, (which determine the strain direction), is $\mathbf{L}_0 = n\mathbf{a}_0 + m\mathbf{b}_0$, where n and m are integers. Under the applied strain the vector $\mathbf{L}_0$ will be deformed to $\mathbf{L}$, so that the vectors $\mathbf{L}$ and $\mathbf{L}_0$ are parallel, i.e. $\mathbf{L}_0$ will be just elongated. The unit cell vectors $\mathbf{a}_0$ and $\mathbf{b}_0$ will be also deformed to $\mathbf{a}$ and $\mathbf{b}$, respectively, so that $\mathbf{L}_0 = n\mathbf{a}_0 + m\mathbf{b}_0 \parallel \mathbf{L} = n\mathbf{a} + m\mathbf{b}$.

If L_0 and $L = L_0 + \delta L$ are the lengths of the vectors $\mathbf{L}_0$ and $\mathbf{L}$, respectively, and $\hat{\boldsymbol{\varepsilon}}$ is the unit vector directed along the strain direction (i.e. $\hat{\boldsymbol{\varepsilon}} = (n\mathbf{a}_0 + m\mathbf{b}_0)/(n^2a_0^2 + m^2b_0^2 + 2nm\mathbf{a}_0\mathbf{b}_0)^{1/2}$, where $b_0 = (b_{x0}^2 + b_{y0}^2)^{1/2}$), then $L = \hat{\boldsymbol{\varepsilon}}(n\mathbf{a} + m\mathbf{b}) = n(\hat{\boldsymbol{\varepsilon}}\mathbf{a}) + m(\hat{\boldsymbol{\varepsilon}}\mathbf{b})$ and $L_0 = \hat{\boldsymbol{\varepsilon}}(n\mathbf{a_0} + m\mathbf{b_0}) = n(\hat{\boldsymbol{\varepsilon}}\mathbf{a_0}) + m(\hat{\boldsymbol{\varepsilon}}\mathbf{b_0})$, i.e. L (L_0) depend on the projections of $\mathbf{a}$, and $\mathbf{b}$ ($\mathbf{a}_0$ and $\mathbf{b}_0$) on the strain direction.

The vectors $\mathbf{a}_0$ and $\mathbf{b}_0$ can be expressed as a sum of bond vectors $\mathbf{r}_{0ai}$ and $\mathbf{r}_{0bi}$, respectively, ($i = 1, 2, 3, ...$), which correspond to specific bonds of the undeformed structure, constituting a crooked line connecting the tails of $\mathbf{a}_0$ and $\mathbf{b}_0$ with their heads, i.e. $\mathbf{a}_0 = \sum_i \mathbf{r}_{0ai}$ and $\mathbf{b}_0 = \sum_i \mathbf{r}_{0bi}$. Thus, if the bond vectors $\mathbf{r}_{0ai}$ and $\mathbf{r}_{0bi}$ are deformed under strain into $\mathbf{r}_{ai}$ and $\mathbf{r}_{bi}$, respectively, then $\mathbf{a} = \sum_i \mathbf{r}_{ai}$ and $\mathbf{b} = \sum_i \mathbf{r}_{bi}$. This is shown schematically in Fig. 2, where the sum of the red colored vectors, (denoted as $\mathbf{r}_{ai}$, $i = 1, 2, 3, ...$), constitute $\mathbf{a}$, while the sum of the green colored vectors, (denoted as $\mathbf{r}_{bi}$, $i = 1, 2, 3, ...$), constitute $\mathbf{b}$. Obviously, the corresponding sums of the projections of $\mathbf{r}_{ai}$ and $\mathbf{r}_{bi}$ along the strain direction equals the projection of $\mathbf{a}$ and $\mathbf{b}$, respectively, along the same direction. These projections of $\mathbf{r}_{ai}$ and $\mathbf{r}_{bi}$ are shown as black arrows in Fig. 2, and should be considered as positive or negative. Thus,

$$\begin{aligned} \delta L &= L - L_0 \\ &= n\sum_i (\hat{\boldsymbol{\varepsilon}}\mathbf{r}_{ai} - \hat{\boldsymbol{\varepsilon}}\mathbf{r}_{0ai}) + m\sum_i (\hat{\boldsymbol{\varepsilon}}\mathbf{r}_{bi} - \hat{\boldsymbol{\varepsilon}}\mathbf{r}_{0bi}), \end{aligned} \tag{8}$$

i.e. δL can be expressed as a function of the differences of the projections of the $\mathbf{r}_{0ai}$, $\mathbf{r}_{ai}$ and the $\mathbf{r}_{0bi}$, $\mathbf{r}_{bi}$ vectors, along the strain direction. We should note that, although the vectors, $\mathbf{a}$, $\mathbf{b}$, $\mathbf{a}_0$, $\mathbf{b}_0$ are not uniquely expressed in terms of bond vectors, the sums of the projections are unique and one could always choose optimal paths (e.g. of minimal length) of bond vectors. Let us now see how the differences of those projections depend on the bond deformations.

B. The strain constrain

Let us assume that strain along a specific direction is applied to a bond, as shown in Fig. 1(b). For convenience we have assumed that the strain direction coincides with the x-axis direction. Let us further assume that at equilibrium for $\varepsilon = 0$, the bond length and the angle between the bond and the strain direction are l_0 and θ_0, and under strain they become $\theta_0+\delta\theta$ and $l_0+\delta l$, respectively. If the projections of the bond along and normal to the strain direction for $\varepsilon = 0$ are x_0 and y_0, respectively, and under strain they are $x_0+\delta x$ and $y_0+\delta y$, respectively, then $x_0 = l_0\cos\theta_0$, $y_0 = l_0\sin\theta_0$, $x_0+\delta x = (l_0+\delta l)\cos(\theta_0+\delta\theta)$ and $y_0+\delta y = (l_0+\delta l)\sin(\theta_0+\delta\theta)$.

Thus the projection of the bond deformation along the strain direction is

$$\delta x \;\approx\; \delta l\cos\theta_0 - l_0\sin\theta_0\delta\theta \tag{9}$$

and the projection normal to the strain direction is

$$\delta y \;\approx\; \delta l\sin\theta_0 + l_0\cos\theta_0\delta\theta. \tag{10}$$

According to Eq. (9), the projection δx of the deformation of $\mathbf{r}_{0ai}$ along the strain direction $\hat{\boldsymbol{\varepsilon}}$ is

$$\begin{aligned}\delta x &= \hat{\boldsymbol{\varepsilon}}\mathbf{r}_{ai} - \hat{\boldsymbol{\varepsilon}}\mathbf{r}_{0ai} \\ &= \delta l_{ai}\cos\theta_{0ai} - l_{0ai}\sin\theta_{0ai}\delta\theta_{ai},\end{aligned} \tag{11}$$

where $l_{0ai} = |\mathbf{r}_{0ai}|$, θ_{0ai} is the angle between $\mathbf{r}_{a0i}$ and the strain direction (i.e. $\cos\theta_{0ai} = \hat{\boldsymbol{\varepsilon}}\mathbf{r}_{0ai}/l_{0ai}$), and δl_{ai} and $\delta\theta_{ai}$ are the deformations of l_{0ai} and θ_{0ai}, respectively. Changing the index "a" with "b", we get the corresponding relation for $\mathbf{r}_{0bi}$. Consequently,

$$\begin{aligned}\delta L &= n\sum_i\left(\delta l_{ai}\cos\theta_{0ai} - l_{0ai}\sin\theta_{0ai}\delta\theta_{ai}\right) + \\ &\quad m\sum_i\left(\delta l_{bi}\cos\theta_{0bi} - l_{0bi}\sin\theta_{0bi}\delta\theta_{bi}\right).\end{aligned} \tag{12}$$

As a function of the projections of independently deformed bonds, this equation is written as

$$\delta L = \sum_i q_i\left(\delta l_i\cos\theta_{0i} - l_{0i}\sin\theta_{0i}\delta\theta_i\right) \tag{13}$$

where here index i is the same as in Eq. (6), (i.e. it runs over the bond vectors of the independently deformed bonds) and q_i is the number of the bond vectors $\mathbf{r}_{0a}$ and $\mathbf{r}_{0b}$ with equivalent deformations, which contribute to the sums in Eq. (8). Obviously, if $\mathbf{r}_i$ does not contribute to the sums in Eq. (8), then $q_i = 0$, and if $-\mathbf{r}_i$ contributes to the sums in (8) instead of $\mathbf{r}_i$, then the angle θ_{0i} of the above equation should be replaced by $\theta_{0i}+\pi$, which changes the sign of both $\cos\theta_{0i}$ and $\sin\theta_{0i}$. This sign change can be absorbed in q_i, and therefore, the constrain of our case has the form

$$\varepsilon - \sum_i q_i\left(\delta l_i\cos\theta_{0i} - l_{0i}\sin\theta_{0i}\delta\theta_i\right)/L_0 = 0. \tag{14}$$

As one can see, the deformation energy in Eq. (6) is expressed as a function of the deformations δl_i and $\delta\phi_{ij}$, while the constrain in Eq. (14) is expressed as a function of δl_i and $\delta\theta_i$. As we show in the Sec. A,

$$\forall\phi_{ij}\in(0,\pi],\quad \delta\phi_{ij}^2 = (\delta\theta_j - \delta\theta_i)^2, \tag{15}$$

and therefore, the function Λ in Eq. (7), which has to be minimized, can be rewritten as

$$\begin{aligned}\Lambda &= \Lambda\left(\{\delta l_i\},\{\delta\theta_i\},\lambda\right) \\ &= \frac{1}{2}\sum_i\left(n_i k_{s,i}\delta l_i^2 + \frac{1}{2}\sum_j m_{ij}k_{b,ij}(\delta\theta_i - \delta\theta_j)^2\right) \\ &\quad +\lambda\left(\varepsilon - \sum_i q_i\left(\delta l_i\cos\theta_{0i} - l_{0i}\sin\theta_{0i}\delta\theta_i\right)/L_0\right),\end{aligned} \tag{16}$$

where by $\{\delta l_i\}$ and $\{\delta\theta_i\}$ we denote all the δl_i and $\delta\theta_i$ independent variables, respectively, (i.e. $\{\delta l_i\} = \delta l_1, \delta l_2, \ldots$ and $\{\delta\theta_i\} = \delta\theta_1, \delta\theta_2, \ldots$), and therefore Λ becomes a function of only δl_i, $\delta\theta_i$ and λ.

It is worth noting that the projection of $\delta\mathbf{L} = \mathbf{L} - \mathbf{L}_0$ normal to the strain direction should be zero, i.e. (according to Eq. (10))

$$\sum_i q_i(\delta l_i\sin\theta_{0i} + l_{0i}\cos\theta_{0i}\delta\theta_i) = 0. \tag{17}$$

As we will see, minimizing Λ in (16) we will be able to calculate the differences of $\delta\theta_i$ for the same atom, (i.e. the bond angle deformations $\delta\phi_{ij}$), but not the deformations $\delta\theta_i$ themselves, which give the direction of the bonds with respect to the strain direction. However, using (17) and the results of the minimization in (16), the deformations $\delta\theta_i$ can be also determined and we can have a complete figure for the deformations of the structure.

III. MINIMIZATION OF $\Lambda(\{\delta l_i\},\{\delta\theta_{ij}\},\lambda)$

The steady state of Λ occurs at the specific δl_i and $\delta\theta_i$ values for which

$$\partial\Lambda/\partial\delta l_i = 0 \qquad \text{and} \qquad \partial\Lambda/\partial\delta\theta_i = 0. \tag{18}$$

δl_i appears only in one term of U, namely in $(1/2)k_{s,i}\delta l_i^2$. Consequently, from $\partial\Lambda/\partial\delta l_i = 0$ we obtain

$$\delta l_i = \frac{\lambda}{L_0}\frac{q_i}{n_i}\frac{\cos\theta_{0i}}{k_{s,i}}. \tag{19}$$

On the other hand, $\delta\theta_i$ appears in 4 terms of U (see Fig. 1(a)), namely in $m_{ij_1}k_{b,ij_1}(\delta\theta_i - \delta\theta_{j_1})^2$ and $m_{ij_2}k_{b,ij_2}(\delta\theta_i - \delta\theta_{j_2})^2$ for the angles $\delta\phi_{ij_1}$ and $\delta\phi_{ij_2}$ of atom A, and $m_{ij_3}k_{b,ij_3}(\delta\theta_i - \delta\theta_{j_3})^2$ and $m_{ij_4}k_{b,ij_4}(\delta\theta_i - \delta\theta_{j_4})^2$ for the angles $\delta\phi_{ij_3}$ and $\delta\phi_{ij_4}$ of atom B. From $\partial\Lambda/\partial\delta\theta_i = 0$ we obtain the linear system

$$\frac{1}{2}\sum_{k=1}^{4} m_{ij_k}k_{b,ij_k}(\delta\theta_i - \delta\theta_{j_k}) = -\lambda q_i l_{0i}\sin\theta_{0i}/L_0. \tag{20}$$

Substituting the expressions for $\delta\theta_i$ obtained from Eq. (20) and the expressions for δl_i shown in Eq. (19) into (14), we obtain an equation for λ. Solving this equation with respect to λ, we obtain λ as a function of the strain ε and the strain angle θ_0.

As we show in the Section B,

$$U_{min} = \lambda\varepsilon/2, \tag{21}$$

where U_{min} is the minimum of U subject to the constrain $\varepsilon = \delta L/L_0$. Thus, if λ is determined, then U_{min} can also be determined. Eq. (21) gives a physical meaning in the Lagrange multiplier λ and minimizes the effort to find a convenient expression for U_{min} as a function of $k_{s,i}$ and $k_{b,ij}$ for strain ε.

IV. INCLUDING SECOND NEAREST NEIGHBOR STRETCHING TERMS

As we can see from Eqs. (19) and (20), the original stick and spiral model, expressed utilizing (6), does not provide any coupling between δl_i and $\delta\phi_{ij}$. However, as already mentioned, including energy terms which describe stretching from second nearest neighbor interactions, we obtain a more accurate model, since it provides coupling between δl_i and $\delta\phi_{ij}$.

Let us assume that atoms B and C are second nearest neighbors, forming bonds i and j, respectively, with atom A. If $\mathbf{r}_{0i}$ and $\mathbf{r}_{0j}$ are the bond vectors of bonds i and j, at equilibrium for $\varepsilon = 0$, then, depending on the orientation of $\mathbf{r}_{0i}$ and $\mathbf{r}_{0j}$, the interatomic distance r_{0ij} between atoms B and C is either the magnitude of the vector $\mathbf{r}_{0j} - \mathbf{r}_{0i}$ (if both heads or tails of $\mathbf{r}_{0i}$ and $\mathbf{r}_{0j}$ are at the position of atom A), or the vector $\mathbf{r}_{0j} + \mathbf{r}_{0i}$ (if the tail of the one and the head of the other are at the position of atom A).

If the interatomic distance r_{0ij} is deformed upon strain by δr_{ij}, then the deformation energy per unit cell U is

$$U = U_1 + U_2 = U_1 + (1/2)\sum_i \sum_j p_{ij}(1/2)k_{s,ij}\delta r_{ij}^2, \tag{22}$$

where U_1 is the deformation energy of the original stick and spiral model in Eq. (6) and U_2 describes the contribution due to stretching deformations of second nearest neighbor interatomic distances. The factor $1/2$ in the second term of Eq. (22) is inserted to avoid double counting, the notation i and j is the same as in (6) and p_{ij} is the number of the equivalent second nearest neighbor interatomic distances in the unit cell with a δr_{ij} deformation. Obviously, $p_{ij} = m_{ij}$, because each specific bond angle ϕ_{ij} corresponds to a specific second nearest neighbor interatomic distance r_{ij}.

Consequently, for the atomic arrangement shown in Fig. 1(a), Eqs. (19) and (20) should be replaced by

$$n_i k_{s,i}\delta l_i + \frac{1}{2}\sum_{k=1}^{4} m_{ij_k} k_{s,ij_k}\delta r_{ij_k}\frac{\partial\delta r_{ij_k}}{\partial\delta l_i} = \lambda q_i \cos\theta_{0i}/L_0 \tag{23}$$

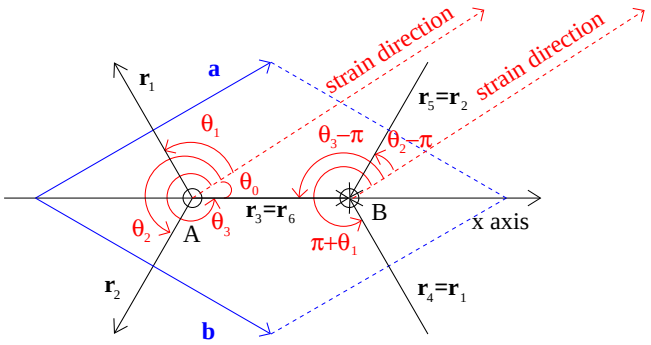

FIG. 3: (Color online) Graphene unit cell. The lattice vectors are $\mathbf{a} = \mathbf{r}_1 - \mathbf{r}_3$ and $\mathbf{b} = \mathbf{r}_1 - \mathbf{r}_2$. The bond vectors for atom A are $\mathbf{r}_1$, $\mathbf{r}_2$ and $\mathbf{r}_3$, while for atom B they are $-\mathbf{r}_1$, $-\mathbf{r}_2$ and $-\mathbf{r}_3$. The bond angles θ_i with respect to the strain direction are also shown.

and

$$\frac{1}{2}\sum_{k=1}^{4} m_{ij_k}\left[k_{b,ij_k}(\delta\theta_i - \delta\theta_{j_k}) + k_{s,ij_k}\delta r_{ij_k}\frac{\partial\delta r_{ij_k}}{\partial\delta\theta_i}\right] = -\lambda q_i l_{0i}\sin\theta_{0i}/L_0, \tag{24}$$

which have to be solved.

As we show in the Sec. C,

$$\begin{aligned} r_{0ij}\delta r_{ij} \;=\; & (l_{0i} \mp l_{0j}\cos(\theta_{0i} - \theta_{0j}))\,\delta l_i \\ & + (l_{0j} \mp l_{0i}\cos(\theta_{0j} - \theta_{0i}))\,\delta l_j \\ & \pm l_{0i}l_{0j}\sin(\theta_{0i} - \theta_{0j})(\delta\theta_i - \delta\theta_j), \end{aligned} \tag{25}$$

and

$$\partial\delta r_{ij}/\partial\delta l_i = \left[l_{0i} \mp l_{0j}\cos(\theta_{0i} - \theta_{0j})\right]/r_{0ij}, \tag{26}$$

$$\partial\delta r_{ij}/\partial\delta\theta_i = \pm l_{0i}l_{0j}\sin(\theta_{0i} - \theta_{0j})/r_{0ij}. \tag{27}$$

The upper signs, (wherever $\pm$ and $\mp$ appear), occur when $\mathbf{r}_i$ and $\mathbf{r}_j$ have their tails (or their heads) at the position of the same atom and the lower signs, when the tail of the one and the head of the other are at the position of the same atom, as explained in Sec. C.

Obviously, if $k_{s,ij} = 0$, then $U_2 = 0$ and the modified stick and spiral model reduces to the original one. Thus, we can treat both models by solving the system of Eqs. (23) and (24) of the modified model. Then, by setting $k_{s,ij} = 0$ in these solutions, we directly get the solutions of (19) and (20) of the original model. This is the subject of the next section specified for graphene.

V. APPLICATION TO GRAPHENE

Bellow, as well as in the appendices, whenever the indices i', j' and k' are used, $(i', j', k') = (1, 2, 3)$, or $(2, 3, 1)$, or $(3, 1, 2)$.

A. The energy

Fig. 3 shows the unit cell of graphene, which is defined by the lattice vectors $\mathbf{a} = (\sqrt{3}/2)(\sqrt{3}\hat{\mathbf{i}} + \hat{\mathbf{j}})a_0$ and $\mathbf{b} = (\sqrt{3}/2)(\sqrt{3}\hat{\mathbf{i}} - \hat{\mathbf{j}})a_0$, where a_0 is the bond length of graphene. In this figure, A and B are the 2 atoms of the lattice base. As one can see, there are 3 bonds per unit cell, which can be deformed independently, corresponding to the bond vectors $\mathbf{r}_1$, $\mathbf{r}_2$ and $\mathbf{r}_3$ of atom A, or the bond vectors $\mathbf{r}_4 = \mathbf{r}_1$, $\mathbf{r}_5 = \mathbf{r}_2$ and $\mathbf{r}_6 = \mathbf{r}_3$ of atom B. Consequently, in Eqs. (6) and (22), $n_i = 1$ ($i = 1, 2, 3$). Moreover, as one can see in Fig. 3, there are six bond angles (with respect to the strain direction) θ_i per unit cell. Three of them correspond to atom A and three to atom B. Since the bond vectors of atom A and B are the same, the angles θ_i corresponding to the bonds of atom A are the same with those corresponding to atom B. Consequently, only three of those six angles can be considered as independently deformed, and $m_{ij} = 2$. Moreover, due to symmetry reasons, $k_{s,i} = k_{s1}$, $k_{s,ij} = k_{s2}$ and $k_{b,ij} = k_b$.

Thus, the energy per unit cell in the original stick and spiral model (according to Eq. (6)) is

$$U = U_1 = \frac{1}{2}k_{s1}\left(\delta l_1^2 + \delta l_2^2 + \delta l_3^2\right) + k_b' a_0^2\left[(\delta\theta_1 - \delta\theta_2)^2 + (\delta\theta_2 - \delta\theta_3)^2 + (\delta\theta_3 - \delta\theta_1)^2\right], \quad (28)$$

where $k_b' = k_b/a_0^2$.

In the unit cell of graphene shown in Fig. 3, there are six second nearest neighbor interatomic distances, namely r_{12}, r_{23}, r_{31}, r_{45}, r_{56} and r_{64}, where $r_{45} = r_{12}$, $r_{56} = r_{23}$ and $r_{64} = r_{31}$. Consequently, there are only three second nearest neighbor interatomic distances, which can be deformed independently and U_2 in Eq. (22) is

$$U_2 = k_{s2}(\delta r_{1,2}^2 + \delta r_{2,3}^2 + \delta r_{3,1}^2), \quad (29)$$

where δr_{ij} are given by (25), and therefore, the energy per atom U in the modified model is $U = U_1 + U_2$.

B. The strain constrain

As a function of the independently deformed bond vectors $\mathbf{r}_i$, the unit cell vectors $\mathbf{a}$ and $\mathbf{b}$ can be written as

$$\mathbf{a} = \mathbf{r}_3 - \mathbf{r}_2 \qquad \text{and} \qquad \mathbf{b} = \mathbf{r}_3 - \mathbf{r}_1. \quad (30)$$

Thus, if $\mathbf{L}_0 = n\mathbf{a} + m\mathbf{b}$ defines the strain direction, then $\mathbf{L}_0 = (n+m)\mathbf{r}_3 - n\mathbf{r}_2 - m\mathbf{r}_1$, and consequently the q_is in (14) are $q_3 = n + m$, $q_2 = -n$ and $q_1 = -m$. As we show in the Sec. D,

$$q_i = 2L_0/(3a_0)\cos\theta_{0i}, \quad (31)$$

where

$$\theta_{0i} = 2\pi i/3 - \theta_0, \quad i = 1, 2, 3, \quad (32)$$

and consequently, (as shown in the same Appendix), the strain constraint of Eq. (14) takes the form

$$\varepsilon = \frac{2}{3a_0}\sum_{j=1}^{3}\cos^2\theta_{0j}\delta l_j - \frac{1}{3}\sum_{j=1}^{3}\sin 2\theta_{0j}(\delta\theta_j - \delta\theta_i), \quad (33)$$

while (17) becomes

$$\delta\theta_i = \sum_{j=1}^{3}\left(\frac{2}{3}\cos^2\theta_{0j}(\delta\theta_i - \delta\theta_j) - \frac{\delta l_j}{3a_0}\sin 2\theta_{0j}\right), \quad (34)$$

respectively, where $i = 1$, or 2, or 3.

C. Solving for the deformations δl_i and $\delta\theta_i$

As we show in the Sec. (E), Eqs. (23) and (24) give

$$(\sqrt{3}/2)k_{s2}\left[\sqrt{3}(2\delta l_{i'} + \delta l_{j'} + \delta l_{k'}) + a_0(\delta\theta_{j'} - \delta\theta_{k'})\right] + k_{s1}\delta l_{i'} = (2\lambda/3a_0)\cos^2\theta_{0i'} \quad (35)$$

and

$$(k_b' + k_{s2}/4)\,a_0^2[(\delta\theta_{i'} - \delta\theta_{j'}) + (\delta\theta_{i'} - \delta\theta_{k'})] + (\sqrt{3}/4)a_0 k_{s2}(\delta l_{k'} - \delta l_{j'}) = -(\lambda/6)\sin 2\theta_{0i'}. \quad (36)$$

The solution of these equations, (as shown in the same appendix), is of the form

$$\delta l_i = 3a_0(\xi_1'\cos^2\theta_{0i} + \xi_2') \quad (37)$$

and

$$\delta\theta_j - \delta\theta_i = \xi_3'(\sin 2\theta_{0i} - \sin 2\theta_{0j}), \quad (38)$$

where $\xi_1' = 8k_b'\lambda/(9a_0^2K')$, $\xi_2' = k_{s2}\lambda(k_{s1} - 18k_b')/[9a_0^2K'(k_{s1}+6k_{s2})]$, $\xi_3' = 2\lambda k_{s1}/(9a_0^2K')$ and $K' = k_{s1}k_{s2} + (4k_{s1} + 6k_{s2})k_b'$. For these expressions of δl_i and $\delta\theta_j - \delta\theta_i$, Eqs. (33) and (34) yield

$$\varepsilon = (9\xi_1' + 12\xi_2' + 2\xi_3')/4 \quad \text{and} \quad \delta\theta_i = -\xi_3'\sin 2\theta_{0i}, \quad (39)$$

(see Sec. E for details). Consequently,

$$\varepsilon = \lambda K_0/[9a_0^2K'(k_{s1} + 6k_{s2})], \quad (40)$$

where $K_0 = k_{s1}^2 + 9k_{s1}k_{s2} + 18(k_{s1}+3k_{s2})k_b'$ and therefore,

$$\lambda = 9a_0^2\varepsilon K'(k_{s1} + 6k_{s2})/K_0. \quad (41)$$

Thus,

$$\delta l_i = 3a_0\lambda_i\varepsilon, \quad \text{and} \quad \delta\theta_j - \delta\theta_i = \mu_{ij}\varepsilon, \quad (42)$$

where

$$\lambda_i = \xi_1\cos^2\theta_{0i} + \xi_2, \quad (43)$$

$$\mu_{ij} = -\mu_{ji} = \xi_3(\sin 2\theta_{0i} - \sin 2\theta_{0j}) \quad (44)$$

and

$$\xi_1 = 8k_b'(k_{s1} + 6k_{s2})/K_0, \tag{45}$$

$$\xi_2 = k_{s2}(k_{s1} - 18k_b')/K_0, \tag{46}$$

$$\xi_3 = 2k_{s1}(k_{s1} + 6k_{s2})/K_0. \tag{47}$$

Using Eq. (H13), (44) gives

$$\mu_{i'j'} = -\mu_{j'i'} = -\sqrt{3}\xi_3 \cos 2\theta_{0k'} \tag{48}$$

Obviously, Eq. (39) leads to

$$9\xi_1 + 12\xi_2 + 2\xi_3 = 4 \quad \text{and} \quad \delta\theta_i = -(\xi_3 \sin 2\theta_{0i})\varepsilon. \tag{49}$$

The former shows that ξ_1, ξ_2 and ξ_3 are not independent.

Moreover, according to the relations between ϕ_{ij} and θ_i shown in Sec. A, the relations between the ϕ_{ij} and θ_i angles of graphene, shown in Fig. 3 are

$$\phi_{21} = \theta_2 - \theta_1, \quad \phi_{32} = \theta_3 - \theta_2 \quad \text{and} \quad \phi_{13} = 2\pi + \theta_1 - \theta_3. \tag{50}$$

Thus, the bond angle deformations $\delta\phi_{ij}$ are

$$\delta\phi_{i'j'} = \delta\phi_{j'i'} = \delta\theta_{j'} - \delta\theta_{i'}. \tag{51}$$

Due to the symmetry of the unit cell, the results we find for strain angle θ_0, will be the same for strain angles $n\pi/3 \pm \theta_0$, $n = 0, 1, 2, 3, 4, 5$. Thus, without loss of generality, we may assume that $0 \le \theta_0 \le \pi/6$.

D. Energy, Young's modulus and Poisson's ratio

According to Eq. (21), the deformation energy per unit cell is $U = \lambda\varepsilon/2$. For graphene, λ is given by (41), and consequently,

$$U = (3a_0\varepsilon)^2 A, \tag{52}$$

where

$$A = (k_{s1} + 6k_{s2})(k_{s1}k_{s2} + (4k_{s1} + 6k_{s2})k_b')/(2K_0). \tag{53}$$

As for the Young's modulus E, it is easy to show that $E = 2U/(V\varepsilon^2)$, where V is the volume of the unit cell ($V = 3\sqrt{3}a_0^2 d_0/2$) and d_0 is the hypothetical depth of the graphene layer, which is assumed to be equal to the graphite interlayer separation ($d_0 = 3.34$Å), in order to direct compare the Young's modulus values of two dimensional (2D) carbon structures with the known values for three dimensional (3D) systems, like graphite[5]. Thus, for the above expression for A,

$$E = 4\sqrt{3}A/d_0, \tag{54}$$

Moreover, in Sec. F we show that the Poisson's ratio ν is

$$\nu = -3\xi_1/4 - 3\xi_2 + \xi_3/2, \tag{55}$$

which for the ξ_1, ξ_2 and ξ_3 expressions of (45), (46) and (47) becomes

$$\nu = [(k_{s1} + 6k_{s2})(k_{s1} - 6k_b') - 3k_{s2}(k_{s1} - 18k_b')]/K_0. \tag{56}$$

As one can see from the above expressions, U, E and ν are independent of the strain angle θ_0, and consequently, graphene is isotropic.

E. Relations between k_{s1}, k_{s2} and k_b' with ξ_1, ξ_2, ξ_3 and A

One would have thought that Eqs. (45), (46) and (47), which form a 3×3 system of equations, would provide solutions for k_{s1}, k_{s2} and k_b' as functions of ξ_1, ξ_2 and ξ_3. However, as shown in Eq. (49), ξ_1, ξ_2 and ξ_3 are not independent, and therefore, these equations can not provide relations for k_{s1}, k_{s2} and k_b' as functions of ξ_1, ξ_2 and ξ_3. On the other hand, A, which is independent of ξ_1, ξ_2 and ξ_3, is also a function of k_{s1}, k_{s2} and k_b'. Therefore, k_{s1}, k_{s2} and k_b' could be written as functions of ξ_1, ξ_2, ξ_3 and A.

As we show in the Sec. G,

$$\frac{k_b'}{k_{s1}} = \frac{\xi_1}{4\xi_3} \quad \text{and} \quad \frac{k_{s2}}{k_{s1}} = \frac{-\xi_2}{1 - \xi_3 + 3\xi_2} \tag{57}$$

and

$$k_{s1} = 4A\left(\frac{1 - \xi_3 + 3\xi_2}{1 - \xi_3 - 3\xi_2}\right)\frac{1}{\xi_1 + 2\xi_2}, \tag{58}$$

$$k_{s2} = -4A\left(\frac{\xi_2}{1 - \xi_3 - 3\xi_2}\right)\frac{1}{\xi_1 + 2\xi_2} \tag{59}$$

and

$$k_b' = A\frac{\xi_1}{\xi_3}\left(\frac{1 - \xi_3 + 3\xi_2}{1 - \xi_3 - 3\xi_2}\right)\frac{1}{\xi_1 + 2\xi_2}. \tag{60}$$

F. The original stick and spiral model

The corresponding results for the original stick and spiral model (i.e. not including second nearest neighbor interactions for stretching) can be obtained by setting $k_{s2} = 0$. Thus, the solution of Eqs. (19) and (20) have again the form of (42), with λ_i and μ_{ij} given again by Eqs. (43) and (44), but now

$$\xi_1 = \frac{8k_b'}{k_{s1} + 18k_b'}, \quad \xi_2 = 0 \quad \text{and} \quad \xi_3 = \frac{2k_{s1}}{k_{s1} + 18k_b'}. \tag{61}$$

The first of the Eqs. (49) becomes $9\xi_1 + 2\xi_3 = 4$, while the second remains the same. The energy and the Young's modulus are again given by (52) and (54), respectively, but now

$$A = 2k_{s1}k_b'/(k_{s1} + 18k_b'), \tag{62}$$

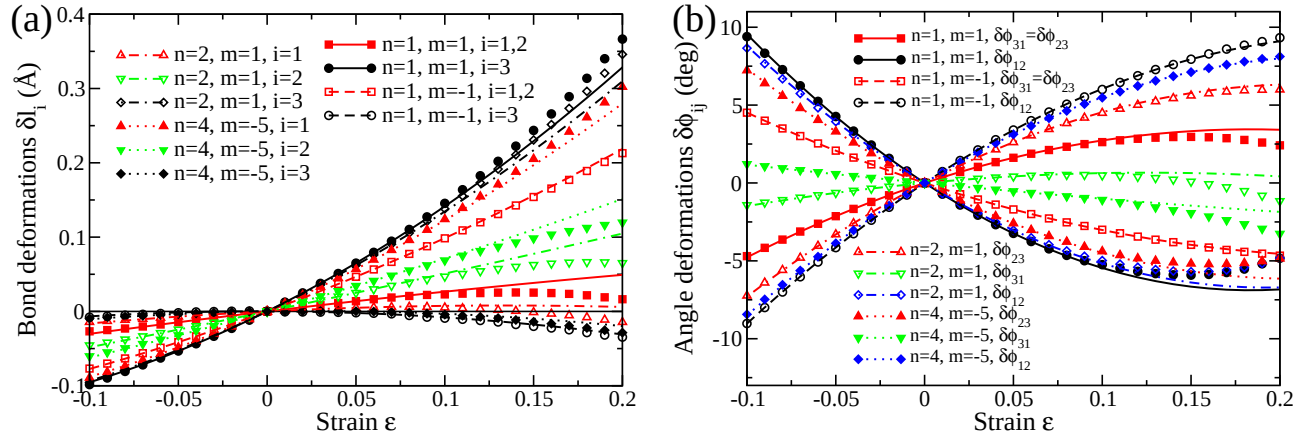

FIG. 4: (Color online) (a) Bond length deformations δl_i and (b) bond angle deformations $\delta\phi_{ij}$ as a function of strain ε, upon stretching along the directions defined by the vectors $\mathbf{L} = n\mathbf{a} + m\mathbf{b}$. $n = 1$ and $m = 1$ corresponds to the arm chair direction. $n = 1$ and $m = -1$ corresponds to the zig-zag direction.

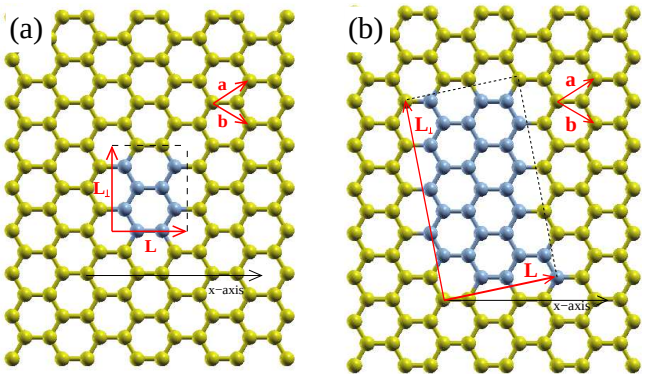

FIG. 5: (Color online) Rectangular unit cells and strain directions used in our calculations. Unit cell atoms are shown with blue color. (a) For strain along the arm chair ($\mathbf{L} = \mathbf{a}+\mathbf{b}$) and the zig-zag ($\mathbf{L}_\perp = \mathbf{a} - \mathbf{b}$) direction, and (b) for strain along the direction of the vectors $\mathbf{L} = 2\mathbf{a} + \mathbf{b}$ and $\mathbf{L}_\perp = 4\mathbf{a} - 5\mathbf{b}$.

and the Poisson's ratio is

$$\nu = (2\xi_3 - 3\xi_1)/4 = (k_{s1} - 6k_{s2})/(k_{s1} + 18k_b'). \quad (63)$$

Moreover, the relations between k_{s1} and k_b', with ξ_1, ξ_3 and A are

$$k_{s1} = 4A/\xi_1 \quad \text{and} \quad k_b' = A/\xi_3. \quad (64)$$

VI. FORCE CONSTANTS FROM DFT RESULTS AND DISCUSSION

A. Details of our DFT calculations

For our DFT calculations we used the Quantum Espresso[48] code at the level of GGA/PBE functional[49] and adopted an ultra-soft pseudopotential for Carbon[50,51]. The two unit cells are shown in Fig. 5. For the rectangular unit cell of Fig. 5(a) we used a 12×12 k-point mesh, while for the unit cell of Fig. 5(b) a 12×6 (12 along the small real space direction). In addition, we used cut-offs 50 and 500 Ryd for the wave functions and charge density, respectively, and occupation smearing of 5 mRyd. As in Ref. 5, for non zero uniaxial strain, the unit cells were extended in the strain direction while all the atoms in the cell as well as the vertical cell dimension were fully relaxed.

B. Results

As a first step, we want to calculate the parameters λ_i and μ_{ij}, which depend on the strain direction, as well as A, which is independent. To calculate the λ_i and μ_{ij} values, we fit the deformations δl_i and $\delta\phi_{ij}$ in the strain range $[-0.05, 0.05]$ to a quadratic form, considering that the coefficient of the linear term represent the corresponding $3a_0\lambda_i$ and μ_{ij} values in Eq. (42), respectively. For the calculation of A, we fit the corresponding energy per atom values to a fourth order polynomial, considering that $(3a_0)^2 A$ is the coefficient of the quadratic term.

Although in real world, graphene sheet bends for negative strains, computationally it is possible to perform calculations for negative strains without bending of the structure. Fitting a curve to the deformations δl_i, $\delta\phi_{ij}$ and U for both negative and the positive strain values, we expect a better estimation of λ_i, μ_{ij} and A values, than using an extrapolation of δl_i, $\delta\phi_{ij}$ and U at $\varepsilon = 0$, which can be obtained from a fitting of the deformation values of δl_i, $\delta\phi_{ij}$ and U for positive strain values only.

Using the DFT method presented above, we calculated the deformations δl_i and $\delta\phi_{ij}$, $i, j = 1, 2, 3$, and the deformation energy per atom U, for uniaxial strain along

n	m	θ_0 (°)	i	θ_{0i} (°)	$\cos^2\theta_{0i}$	λ_i	$\cos 2\theta_{0i'}$	$\mu_{j'k'}$
1	-1	90.000000	3	270.000000	0.000000	-0.001556	-1.000000	1.315279
4	-5	100.893395	3	259.106605	0.035714	0.008633	-0.928571	1.221761
2	1	10.893395	1	109.106605	0.107143	0.027796	-0.785714	1.032964
1	1	0.000000	1, 2	120.000000	0.250000	0.066506	-0.500000	0.654704
2	1	10.893395	2	229.106605	0.428571	0.116258	-0.142857	0.185116
4	-5	100.893395	2	139.106605	0.571429	0.156141	0.142857	-0.190542
1	-1	90.000000	1, 2	30.000000	0.750000	0.206426	0.500000	-0.657640
4	-5	100.893395	1	19.106605	0.892857	0.246905	0.785714	-1.031171
2	1	10.893395	3	349.106605	0.964286	0.267113	0.928571	-1.218509
1	1	0.000000	3	360.000000	1.000000	0.277621	1.000000	-1.309408

TABLE I: Values of λ_i, μ_{ij} and A obtained from the fittings for the four strain directions.

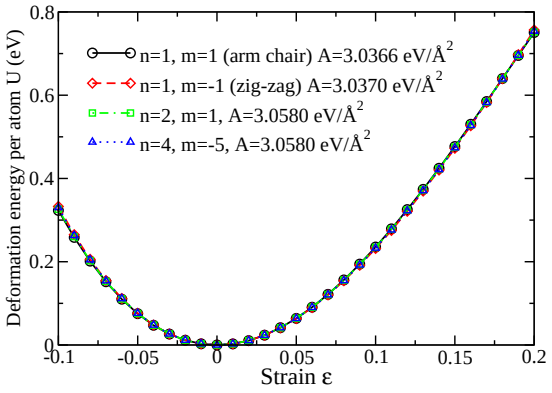

FIG. 6: (Color online) Deformation energy per atom for strain along the direction of the vectors $\mathbf{L} = n\mathbf{a} + m\mathbf{b}$, for n and m shown in the legends. For each strain direction, the A values of (52) are also presented in the legends.

the high symmetry arm chair and zig-zag directions, as well as the directions along the vectors $\mathbf{L} = 2\mathbf{a} + \mathbf{b}$ and $\mathbf{L}_\perp = 4\mathbf{a} - 5\mathbf{b}$, which are perpendicular to each other, and randomly selected. We increase the strain gradually with a 0.01 strain step in the range between $\varepsilon = -0.1$ and $\varepsilon = 0.25$. The results are presented in Figs. 4 and 6, respectively. The fitting functions are presented in the Supplementary Data.

The values of λ_i and μ_{ij} obtained from the fits for the four strain directions are presented in Table I, while the corresponding A values are shown in the legends of Fig. 6. Although A was expected to be independent of the strain direction, the values of A shown in Fig. 6 does not seem to agree with this prediction. However, this discrepancy is due to numerical errors introduced from the different unit cells used. The total energy per atom difference between the equilibrium graphene geometries at $\varepsilon = 0$ obtained using the two unit cells of Fig. 5 is 2.3×10^{-4} eV/atom. As one can show, this difference is enough to produce such a discrepancy in A, (i.e. of the order of 10^{-3} eV/Å^2). It is worth noting, however, that the difference between the two A values, corresponding to the two perpendicular strain directions of the same unit cell, is of the order of 10^{-4} eV/Å^2. For our calculations we will adopt the value $A = 3.046$ eV/Å^2, which corresponds to an average of the obtained values.

The second step is to calculate the values of ξ_1, ξ_2 and ξ_3 using the λ_i and μ_{ij} values of Table I and Eqs. (43) and (44). According to these equations, ξ_1, ξ_2 and ξ_3 can be obtained using a linear fitting of the λ_i values as a function of $\cos^2\theta_{0i}$ and the $-\mu_{i'j'}/\sqrt{3}$ values as a function of $\cos 2\theta_{0k'}$. The values of λ_i as a function of $\cos^2\theta_{0i}$ and the values of $-\mu_{i'j'}/\sqrt{3}$ as a function of $\cos 2\theta_{0k'}$, as well as the corresponding fitting lines are shown in Fig. 7(a). The smoothness of the fitting is obvious. These fitting lines are

$$\lambda_i = 0.278912\cos^2\theta_{0i} - 0.002272 \tag{65}$$

and

$$\mu_{i'j'} = -0.758145\sqrt{3}\cos 2\theta_{0k'}. \tag{66}$$

Thus, $\xi_1 = 0.278921$, $\xi_2 = -0.002272$ and $\xi_3 = 0.758145$. Using these values, the value of A, and Eqs. (57) - (60), we can calculate the values of k_{s1}, k_{s2} and k'_b, as well as the ratios k_{s2}/k_{s1} and k'_b/k_{s1}. Thus, $k'_b/k_{s1} = 0.091975$, $k_{s2}/k_{s1} = 0.0096665$, $k_{s1} = 41.972$ eV/Å, $k_{s2} = 0.40572$ eV/Å and $k'_b = 3.8604$ eV/Å. Therefore, roughly speaking $k'_b \approx 0.1k_{s1}$ and $k_{s2} \approx 0.01k_{s1}$, which qualitatively provides the relative strength of each deformation mode. Moreover, according to (54) and (55), $E = 1012$ GPa and $\nu = 0.1744$, in agreement with the results of our previous work[5] obtained fitting the stress σ and the the transverse strain $\varepsilon_\perp$ values as a function of strain, to a third and second order polynomial, respectively.

Knowing the k_{s1}, k_{s2} and k'_b values, we have the ability to predict any mechanical property related to the in-plane deformations of graphene and not only E and ν. For instance, the corresponding biaxial isotropic modulus $E_B = \sigma/\varepsilon$, where $\sigma = \sigma_{xx} = \sigma_{yy}$ and $\varepsilon = \varepsilon_{xx} = \varepsilon_{yy}$, is $E_B = 4\sqrt{3}A'/d_0$, where for the biaxial isotropic deformation $U = 9a_0^2A'\varepsilon^2$. Using (28) and (29), it is easy to show that for biaxial isotropic strain $A' = k_{s1}/6 + k_{s2}$. Thus,

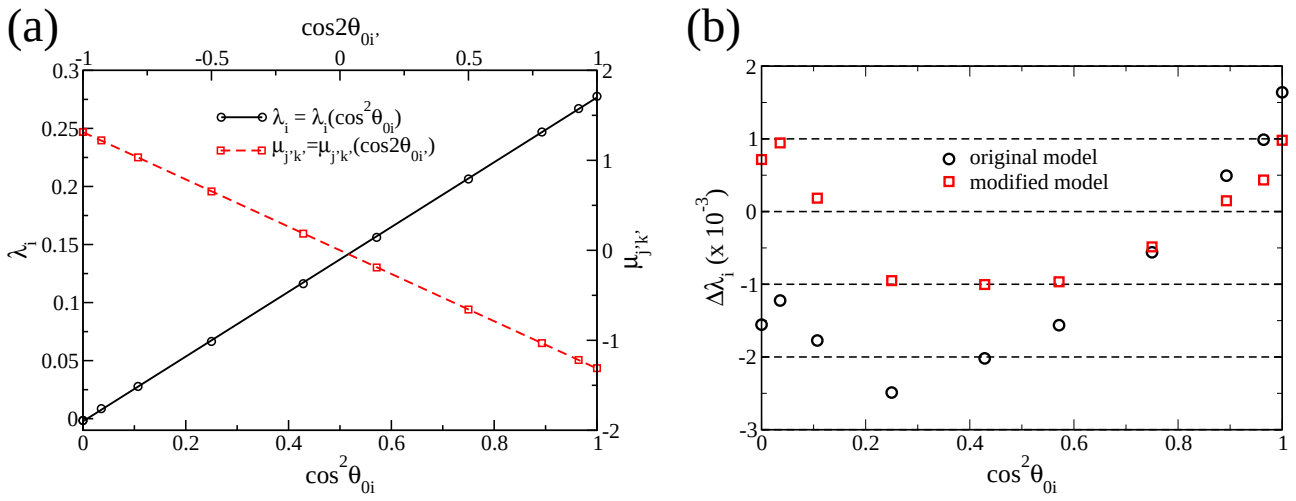

FIG. 7: (Color online) (a) λ_i and $\mu_{j'k'}$ as a function of $\cos^2\theta_{0i}$ and $\cos 2\theta_{0i'}$, respectively and the fitting lines, according to (43) and (48). (b) Difference $\Delta\lambda_i$ between the values λ_i of Table I and those predicted by fitting equations of λ_i as a function of $\cos^2\theta_{0i}$.

for graphene, $E_B = 2459$ GPa. A different calculation using the relation $U = k\delta l^2/2 + k(\delta l + \delta l_\perp)^2/2 = k\delta l^2(1+\nu+\nu^2/2) = 2U_u(1+\nu+\nu^2/2)$, or $A' = 2(1+\nu+\nu^2/2)A$, yields $E_B = 2408$ GPa. As one can see, the two results are very close to each other.

Obviously, the term U_2 corresponding to the stretching of the second nearest neighbor interatomic distances is the less important energy contribution, but it is not a term that can be ignored. If this term is ignored, (which is equivalent to set $k_{s2} = 0$ or $\xi_2 = 0$), the energy model reduces to the original stick and spiral model, which, according to (19), predicts that any bond which is perpendicular to the strain direction remains undeformed. This, however, is in contrast to what we find from our DFT calculations for the l_3 bond length under uniaxial strain along the zig-zag direction. Just for comparison, we also calculate the corresponding ξ_1, ξ_3, k_{s1} and k'_b values obtained from the original stick and spiral morel. Obviously, the form of Eq. (44) does not change in the original stick and spiral model and consequently the value of ξ_3 remains the same as the modified model. However, (43) becomes $\lambda_i = \xi_1 \cos^2\theta_{0i}$. The corresponding fit for the λ_i values of Table I as a function of $\cos^2\theta_{0i}$ yelds $\xi_1 = 0.275981$. In Fig. 7(b) we show the prediction error $\delta\lambda_i$ (i.e. the difference between the λ_i provided by the fitting equations of λ_i as a function of $\cos^2\theta_{0i}$ and the corresponding λ_i values of Table I for the original and the modified stick and spiral model. As we can see, the error for the modified sick and spiral model is between ± 0.001, while the error for the original model is almost double, ranging between -0.0025 and 0.0017. The values of k_{s1} and k'_b for the original model, according to (64) are $k_{s1} = 44.178$ eV/Å and $k'_b = 4.0177$ eV/Å, i.e. they are overesimated by 5 and 4%, respectively, in comparisson with the corresponding values obtained from the modified model. Thus, the original stick and spiral model can not provide an accurate description for the bond and angle deformations of graphene, or at least, it can not provide such an accurate description as the modified model, which is presented here.

VII. CONCLUSIONS

In summary, we present a method for the study of the equilibrium deformations of 2D planar materials under uniaxial strain. The method is based on the stick and spiral model including angle bending energy terms and either only 1st nearest neighbors bond stretching terms (case 1) or both 1st and 2nd nearest neighbors terms (case 2). The method can be generalized to describe structural deformations not only under uniaxial strain, but also under any strain conditions. We present analytic expressions/equations for the structure deformations under strain, namely the equilibrium angle bending and bond stretching deformations for both case 1 (equations (19) and (20)) and case 2 (equations (23) and (24)). We then focus on graphene in order to assess the applicability of our method for which we perform DFT calculations for several values of strain in 4 different directions. We find that the original stick and spiral model (case 1) decouples the equations yielding δl_i from those yielding $\delta\theta_i$ and for graphene, it predicts that the vertical to the strain bonds are not modified. This is in contrast with the DFT results. The inclusion of 2nd nearest neighbors stretching terms (case 2) results in the coupling of δl_i and $\delta\theta_i$, improves the model significantly and brings the results in close agreement with DFT. Our method provides a simple and solid method to study the structural deformations of Graphene in the case of uniaxial strain on

any direction in the elastic regime. The elastic properties of graphene under strain are very accurately reproduced by our method. Although this first application concerns graphene, our method can be applied to any 2D planar material and it would be interesting to assess its accuracy on different structures and materials like Graphene planar allotropes, h-BN, Si_3B, Si_2BN, CdS, etc.

Acknowledgements

NNL acknowledges support from the Hellenic Ministry of Education (through ESPA) and from the GSRT through "Advanced Materials and Devices" program (MIS:5002409).

Appendix A: Relation between ϕ_{ij} and θ_is

Let us define, for each atom of the unit cell, a local anti-clockwise frame of coordinates with its origin at the position of that atom and its x-axis along the strain direction, as shown in Fig. 1(c). Let us denote as $\mathbf{r}_1$, $\mathbf{r}_2$ and $\mathbf{r}_3$ the three bond vectors, which have their tail on atom i and by θ_1, θ_2 and θ_3 the corresponding angles between these bond vectors with the strain direction, respectively, as shown in Fig. 1(c).

Obviously, $\mathbf{r_i r_j} = r_i r_j \cos\phi_{ij}$, where ϕ_{ij} is the angle formed by the bonds i and j, and $\mathbf{r}_i = r_i\cos\theta_i\hat{\mathbf{i}} + r_i\sin\theta_i\hat{\mathbf{j}}$, $i = 1, 2, 3$. Thus, the dot product $\mathbf{r_i r_j}$ can be written as

$$\begin{aligned}\mathbf{r_i r_j} &= (r_i\cos\theta_i\hat{\mathbf{i}} + r_i\sin\theta_i\hat{\mathbf{j}})(r_j\cos\theta_j\hat{\mathbf{i}} + r_j\sin\theta_j\hat{\mathbf{j}}) \\ &= r_i r_j\cos(\theta_j - \theta_i), \end{aligned} \tag{A1}$$

and consequently,

$$\cos\phi_{ij} = \cos(\theta_j - \theta_i) \tag{A2}$$

If ϕ_{0ij}, θ_{0i} and θ_{0j} are the values of the corresponding ϕ_{ij}, θ_i and θ_j angles at equilibrium for $\varepsilon = 0$, then using a first order Taylor expansion around these values, Eq. (A2) yields

$$\sin\phi_{0ij}\delta\phi_{ij} = \sin(\theta_{0j} - \theta_{0i})(\delta\theta_j - \delta\theta_i), \tag{A3}$$

where $\phi_{ij} = \phi_{0ij} + \delta\phi_{ij}$, $\theta_i = \theta_{0i} + \delta\theta_i$ and $\theta_j = \theta_{0j} + \delta\theta_j$ are the corresponding angles at $\varepsilon \neq 0$. Thus, the derivative of $\delta\phi_{ij}$ with respect to $\delta\theta_i$ is

$$\partial\delta\phi_{ij}/\partial\delta\theta_i = \sin(\theta_{0i} - \theta_{0j})/\sin\phi_{0ij}. \tag{A4}$$

Imposing that $0 < \phi_{ij} \leq \pi$, (A2) gives

$$-2k\pi < \pm|\theta_i - \theta_j| \leq (1-2k)\pi. \tag{A5}$$

If θ_is, $i = 1, 2, 3$ are defined inside the same unit circle (e.g. $0 \leq \theta_i < 2\pi$ or $-\pi < \theta_i \leq \pi$), then $-2\pi < \theta_i - \theta_j < 2\pi$. However, according to (A5), $\theta_i - \theta_j$ is out of the range $(-2\pi, 2\pi)$, for $k \neq 0$ or 1, and therefore only $k = 0$ and $k = 1$ should be considered. Consequently, (i) for $k = 0$ (or $0 < |\theta_i - \theta_j| \leq \pi$, according to (A5)), $\phi_{ij} = |\theta_i - \theta_j|$ and (ii) for $k = 1$ (or $\pi \leq |\theta_i - \theta_j| < 2\pi$, according to (A5)), $\phi_{ij} = 2\pi - |\theta_i - \theta_j|$. Thus, for any case, $\delta\phi_{ij} = \pm(\delta\theta_i - \delta\theta_j)$, which leads to (15).

If $\mathbf{r}_i$s, $i = 1, 2, 3$, have their tail at the position of an atom A, then they have their head at the position of the atoms which form bonds with atom A. Assume B is such an atom, which forms a bond with another atom C (different than A), and $\mathbf{r}_1$ and $\mathbf{r}_4$ are the bond vectors corresponding to the bonds A-B and B-C, respectively. There are two options for the direction of $\mathbf{r}_4$: either its head is on the position of atom B and its tail on the position of atom C, or the opposite. In the former case, the relations between the bond angle ϕ_{ij} and the bond angle θ_i with respect to the strain direction are the same with those presented above, since $\mathbf{r}_1\mathbf{r}_4 = r_1 r_4\cos\phi_{14}$. However, in the later case, $\mathbf{r}_1\mathbf{r}_4 = r_1 r_4\cos\omega_{14}$, where the bond angle ϕ_{14} is $\phi_{14} = \pi - \omega_{14}$. Thus, for this case, the relations presented above will be valid if ϕ_{ij} is replaced by $\pi - \phi_{ij}$. Thus, (A2), should be replaced by

$$\cos\phi_{ij} = -\cos(\theta_i - \theta_j), \tag{A6}$$

$$\sin\phi_{0ij}\delta\phi_{ij} = -\sin(\theta_{0j} - \theta_{0i})(\delta\theta_j - \delta\theta_i), \tag{A7}$$

and

$$\partial\delta\phi_{ij}/\partial\delta\theta_i = -\sin(\theta_{0i} - \theta_{0j})/\sin\phi_{0ij}. \tag{A8}$$

If $0 \leq \pi - \phi_{ij} < \pi$, then $0 < \phi_{ij} \leq \pi$. For ϕ_{ij} in this range, (A6) yields (i) if $0 < |\theta_i - \theta_j| \leq \pi$, then $\phi_{ij} = \pi - |\theta_i - \theta_j|$ and (ii) if $\pi < |\theta_i - \theta_j| \leq 2\pi$, then $\phi_{ij} = |\theta_i - \theta_j| - \pi$. Obviously, therefore, for this case, $\delta\phi_{ij}$ is also $\delta\phi_{ij} = \pm(\delta\theta_i - \delta\theta_j)$ and consequently, (15) is also valid.

Appendix B: The physical meaning of λ

Obviously, Λ is parametrically dependent on ε, i.e. $\Lambda = \Lambda(\{\delta l_i\}, \{\delta\theta_i\}, \lambda; \varepsilon)$. If Λ is minimized for $\delta l_i = \delta l_i^*$, $\delta\theta_i = \delta\theta_i^*$, and $\lambda = \lambda^*$, where δl_i^*s, $\delta\theta_i^*$s and λ^* are specific values of δl_is, $\delta\theta_i$s and λ, respectively, then $\Lambda_{min} = \Lambda(\{\delta l_i^*\}, \{\delta\theta_i^*\}, \lambda^*; \varepsilon) = \Lambda_{min}(\varepsilon)$, where Λ_{min} is the minimum of Λ.

For $\delta l_i = \delta l_i^*$ and $\delta\theta_i = \delta\theta_i^*$, the strain ε is $\varepsilon = \delta L(\{\delta l_i^*\}, \{\delta\theta_i^*\})/L_0$ and U is minimized subject to the constrain $\varepsilon = \delta L/L_0$. Thus, if U_{min} is the minimum of U subject to the constrain $\varepsilon = \delta L/L_0$, then $U_{min} = U(\{\delta l_i^*\}, \{\delta\theta_i^*\})$ and (according to (14)), $U(\{\delta l_i^*\}, \{\delta\theta_i^*\}) = \Lambda(\{\delta l_i^*\}, \{\delta\theta_i^*\}, \lambda^*; \varepsilon)$, or $U_{min}(\varepsilon) = \Lambda_{min}(\varepsilon)$.

According to (19) and (20), for the minimized Λ, δl_i^* and $\delta\theta_i^*$ depend linearly on λ^*, and therefore, according to (14), λ^* should depend linearly on ε. Thus, $\delta l_i^* = \delta l_i^*(\varepsilon)$ and $\delta\theta_i^* = \delta\theta_i^*(\varepsilon)$, and consequently, $U_{min} = U_{min}(\varepsilon)$. On the other hand, U_{min} is quadratically dependent on δl_i^* and $\delta\theta_i^*$, and consequently U_{min} should

depend quadratically on ε. Therefore we can write $U_{min}(\varepsilon) = K\varepsilon^2$, where $K = K(\{k_{si}\}, \{k_{bij}\})$.

Obviously, $\partial\Lambda(\{\delta l_i\}, \{\delta\theta_i\}, \lambda; \varepsilon)/\partial\varepsilon = \lambda$, and consequently, $d\Lambda_{min}/d\varepsilon = d\Lambda(\{\delta l_i^*\}, \{\delta\theta_i^*\}, \lambda^*; \varepsilon)/d\varepsilon = \lambda^*$. Since, $\Lambda_{min} = U_{min}$, we have $d\Lambda_{min}/d\varepsilon = dU_{min}/d\varepsilon = 2K\varepsilon$. Thus, $2K\varepsilon = \lambda^*$, which leads to (21).

Appendix C: δr_{ij} as a function of bond length and bond angle deformations

Let us assume that atoms A, B and C belong to the same planar 2D structure and atom A forms bonds with atoms B and C. Let us also assume that $\mathbf{r}_{0i}$ and $\mathbf{r}_{0j}$ are the bond vectors corresponding to the bonds A-B and A-C at equilibrium for $\varepsilon = 0$, having both their tails (or their heads) at the position of atom A. Then the interatomic distance r_{0ij} between atoms B and C is the length of the vector $\mathbf{r}_{0ij} = \mathbf{r}_{0j} - \mathbf{r}_{0i}$, for which

$$r_{0ij}^2 = l_{0i}^2 + l_{0j}^2 - 2l_{0i}l_{0j}\cos\phi_{0ij}. \quad \text{(C1)}$$

where l_{0i} and l_{0j} are the lengths of $\mathbf{r}_{0i}$ and $\mathbf{r}_{0j}$, respectively, and ϕ_{0ij} the bond angle between bonds A-B and A-C. If at the equilibrium state under strain, l_{0i}, l_{0j}, r_{0ij} and ϕ_{0ij} are deformed to $l_i = l_{0i} + \delta l_i$, $l_j = l_{0j} + \delta l_j$, $r_{ij} = r_{0ij} + \delta r_{ij}$ and $\phi_{ij} = \phi_{0ij} + \delta\phi_{ij}$, respectively, then

$$\begin{aligned} r_{ij}^2 &= (l_{0i} + \delta l_i)^2 + (l_{0j} + \delta l_j)^2 \\ &\quad -2(l_{0i} + \delta l_i)(l_{0j} + \delta l_j)\cos(\phi_{0ij} + \delta\phi_{ij}) \\ &\approx l_{0i}^2 + 2l_{0i}\delta l_i + l_{0j}^2 + 2l_{0j}\delta l_j \\ &\quad -2(l_{0i}l_{0j} + l_{0i}\delta l_j + l_{0j}\delta l_i)(\cos\phi_{0ij} - \sin\phi_{0ij}\delta\phi_{ij}) \\ &\approx r_{0ij}^2 + 2(l_{0i}\delta l_i + l_{0j}\delta l_j - l_{0i}\cos\phi_{0ij}\delta l_j \\ &\quad -l_{0j}\cos\phi_{0ij}\delta l_i + l_{0i}l_{0j}\sin\phi_{0ij}\delta\phi_{ij}). \end{aligned} \quad \text{(C2)}$$

For $\delta r_{ij} << r_{0ij}$, $r_{ij}^2 \approx r_{0ij}^2 + 2r_{0ij}\delta r_{ij}$, and consequently, (C2) leads to

$$\begin{aligned} r_{0ij}\delta r_{ij} &= (l_{0i} - l_{0j}\cos\phi_{0ij})\,\delta l_i + (l_{0j} - l_{0i}\cos\phi_{0ij})\,\delta l_j \\ &\quad + l_{0i}l_{0j}\sin\phi_{0ij}\delta\phi_{ij}. \end{aligned} \quad \text{(C3)}$$

Therefore, δr_{ij} is a function of the deformations of δl_i, δl_j, $\delta\theta_i$ and $\delta\theta_j$, (see Sec. A).

The derivatives of δr_{ij} with respect to δl_i and $\delta\theta_i$ are

$$\partial\delta r_{ij}/\partial\delta l_i = [l_{0i} - l_{0j}\cos\phi_{0ij}]\,/r_{0ij} \quad \text{(C4)}$$

and

$$\partial\delta r_{ij}/\partial\delta\theta_i = [l_{0i}l_{0j}\sin\phi_{0ij}/r_{0ij}]\,(\partial\delta\phi_{ij}/\partial\delta\theta_i). \quad \text{(C5)}$$

Using (A2), (A3) and (A4) the above equations give

$$\begin{aligned} r_{0ij}\delta r_{ij} &= (l_{0i} - l_{0j}\cos(\theta_{0i} - \theta_{0j}))\,\delta l_i \\ &\quad + (l_{0j} - l_{0i}\cos(\theta_{0j} - \theta_{0i}))\,\delta l_j \\ &\quad + l_{0i}l_{0j}\sin(\theta_{0i} - \theta_{0j})(\delta\theta_i - \delta\theta_j), \end{aligned} \quad \text{(C6)}$$

and

$$\partial\delta r_{ij}/\partial\delta l_i = [l_{0i} - l_{0j}\cos(\theta_{0i} - \theta_{0j})]\,/r_{0ij}, \quad \text{(C7)}$$

$$\partial\delta r_{ij}/\partial\delta\theta_i = l_{0i}l_{0j}\sin(\theta_{0i} - \theta_{0j})/r_{0ij}. \quad \text{(C8)}$$

However, if the head of $\mathbf{r}_i$ and the tail of $\mathbf{r}_j$ (or vice versa) are at the position of atom A, then we have to use (A6), (A7) and (A8) instead of (A2), (A3) and (A4) (see Sec. A), and thus, (C3), (C4) and (C5) give

$$\begin{aligned} r_{0ij}\delta r_{ij} &= (l_{0i} + l_{0j}\cos(\theta_{0i} - \theta_{0j}))\,\delta l_i \\ &\quad + (l_{0j} + l_{0i}\cos(\theta_{0j} - \theta_{0i}))\,\delta l_j \\ &\quad - l_{0i}l_{0j}\sin(\theta_{0i} - \theta_{0j})(\delta\theta_i - \delta\theta_j), \end{aligned} \quad \text{(C9)}$$

and

$$\partial\delta r_{ij}/\partial\delta l_i = [l_{0i} + l_{0j}\cos(\theta_{0i} - \theta_{0j})]\,/r_{0ij}, \quad \text{(C10)}$$

$$\partial\delta r_{ij}/\partial\delta\theta_i = -l_{0i}l_{0j}\sin(\theta_{0i} - \theta_{0j})/r_{0ij}. \quad \text{(C11)}$$

Commuting i with j in (C4), (C5), (C7), (C8), (C10) and (C11), we obtain the corresponding relations for $\partial\delta r_{ij}/\partial\delta\theta_j$ and $\partial\delta r_{ij}/\partial\delta l_j$.

Appendix D: Derivation of Eqs. (31), (33) and (34)

If $\mathbf{L}_0 = n\mathbf{a} + m\mathbf{b}$ defines the strain direction, then $\mathbf{L}_0 = (\sqrt{3}/2)(\sqrt{3}(n+m)\hat{\mathbf{i}} + (n-m)\hat{\mathbf{j}})a_0$, and consequently, $\cos\theta_0 = 3(n+m)a_0/(2L_0)$ and $\sin\theta_0 = \sqrt{3}(n-m)a_0/(2L_0)$, where θ_0 is the angle of the strain direction with respect to the x-axis. Solving these two equations with respect to n and m, we obtain, $n = 2L_0/(3a_0)((1/2)\cos\theta_0 + (\sqrt{3}/2)\sin\theta_0) = -2L_0/(3a_0)\cos\theta_{02}$ and $m = 2L_0/(3a_0)((1/2)\cos\theta_0 - (\sqrt{3}/2)\sin\theta_0) = -2L_0/(3a_0)\cos\theta_{01}$, and consequently, $n+m = 2L_0/(3a_0)\cos\theta_0 = 2L_0/(3a_0)\cos\theta_{03}$, which lead to (31). In Sec. H we present useful relations between the trigonometric functions of these angles, which will be used here.

Bearing in mind that in graphene $l_{01} = l_{02} = l_{03} = a_0$, and using (31), (14) becomes

$$\varepsilon = \frac{2}{3a_0}\sum_{i=1}^{3}\cos^2\theta_{0i}\delta l_i - \frac{1}{3}\sum_{i=1}^{3}\sin 2\theta_{0i}\delta\theta_i. \quad \text{(D1)}$$

Using (H2) for $k = 2$ of Sec. H, the above equation leads to Eq. (33).

Moreover, (17) becomes

$$\begin{aligned} &\sum_j \cos\theta_{0j}(\delta l_j\sin\theta_{0j} + a_0\cos\theta_{0j}\delta\theta_j) = 0 \Rightarrow \\ &\sum_j (\delta l_j\sin 2\theta_{0j}/2 + a_0\cos^2\theta_{0j}\delta\theta_j) = 0 \Rightarrow \\ &\sum_j (\delta l_j\sin 2\theta_{0j}/2 + a_0\cos^2\theta_{0j}(\delta\theta_j - \delta\theta_i)) = \\ &\qquad = -a_0\delta\theta_i\sum_j\cos^2\theta_{0j} \Rightarrow \\ &\sum_j (\delta l_j\sin 2\theta_{0j} + 2a_0\cos^2\theta_{0j}(\delta\theta_j - \delta\theta_i)) = -3a_0\delta\theta_i, \end{aligned}$$

which leads to (34). In the last step of the above equation we used (H3) of the Sec. H.

Appendix E: Derivation of Eqs. (35), (36), (37), (38) and (39)

As we can see in Fig. 3, the tails of the bond vectors $\mathbf{r}_1$, $\mathbf{r}_2$ and $\mathbf{r}_3$ are at the position of atom A, while the heads of the bond vectors $\mathbf{r}_4$, $\mathbf{r}_5$ and $\mathbf{r}_6$ are at the position of atom B. Therefore, to apply (25), (26) and (27) to (23) and (24), we have to use the upper signs among $\pm$ and $\mp$. Moreover, $l_{0i} = a_0$, $r_{0ij} = \sqrt{3}a_0$, $\cos(\theta_{0j'} - \theta_{0i'}) = \cos(2\pi/3) = -1/2$ and $\sin(\theta_{0j'} - \theta_{0i'}) = \sin(2\pi/3) = \sqrt{3}/2$. Consequently, (25), (26) and (27) yield

$$\delta r_{i',j'} = (\sqrt{3}/2)(\delta l_{i'} + \delta l_{j'}) + (a_0/2)(\delta\theta_{j'} - \delta\theta_{i'}), \quad \text{(E1)}$$

$\partial\delta r_{ij}/\partial\delta l_i = \sqrt{3}/2$ and $\partial\delta r_{i'j'}/\partial\delta\theta_{i'} = -\partial\delta r_{i'j'}/\partial\delta\theta_{j'} = -a_0/2$, respectively. Thus, (23) gives

$$\begin{aligned}
&k_{s1}\delta l_i + \frac{\sqrt{3}}{2}k_{s2}\sum_{k=1}^{4}\delta r_{ij_k} = \frac{\lambda q_i\cos\theta_{0i}}{L_0} \Rightarrow \\
&k_{s1}\delta l_i + \frac{\sqrt{3}}{2}k_{s2}2(\delta r_{ij} + \delta r_{ki}) = \frac{2L_0\cos\theta_{0i}}{3a_0}\frac{\lambda\cos\theta_{0i}}{L_0} \Rightarrow \\
&k_{s1}\delta l_{i'} + \sqrt{3}k_{s2}\left[\frac{\sqrt{3}}{2}(\delta l_{i'} + \delta l_{j'}) + \frac{a_0}{2}(\delta\theta_{j'} - \delta\theta_{i'}) + \right. \\
&\left.\frac{\sqrt{3}}{2}(\delta l_{k'} + \delta l_{i'}) + \frac{a_0}{2}(\delta\theta_{i'} - \delta\theta_{k'})\right] = \frac{2\lambda}{3a_0}\cos^2\theta_{0i'},
\end{aligned}$$

which leads to (35), and (24) gives

$$\begin{aligned}
&2k_b'a_0^2[(\delta\theta_i - \delta\theta_j) + (\delta\theta_i - \delta\theta_k)] + \\
&\quad 2k_{s2}[\delta r_{ij}(\partial\delta r_{ij}/\partial\delta\theta_i) + \delta r_{ki}(\partial\delta r_{ki}/\partial\delta\theta_i)] = \\
&\quad = -\lambda q_i a_0\sin\theta_{0i}/L_0 \Rightarrow \\
&2k_b'a_0^2[(\delta\theta_i - \delta\theta_j) + (\delta\theta_i - \delta\theta_k)] + a_0k_{s2}(\delta r_{ki} - \delta r_{ij}) = \\
&\quad = -\lambda(2L_0\cos\theta_{0i})/(3a_0)a_0\sin\theta_{0i}/L_0 \Rightarrow \\
&k_b'a_0^2[(\delta\theta_{i'} - \delta\theta_{j'}) + (\delta\theta_{i'} - \delta\theta_{k'})] + \\
&\quad a_0k_{s2}/2[(\sqrt{3}/2)(\delta l_{k'} + \delta l_{i'}) + (a_0/2)(\delta\theta_{i'} - \delta\theta_{k'}) - \\
&\quad (\sqrt{3}/2)(\delta l_{i'} + \delta l_{j'}) - (a_0/2)(\delta\theta_{j'} - \delta\theta_{i'})] = \\
&\quad = -(\lambda/6)\sin 2\theta_{0i'},
\end{aligned} \quad \text{(E2)}$$

which leads to (36). Summing up the three equations (35) (i.e. for $(i', j', k') = (1, 2, 3)$, $(2, 3, 1)$ and $(3, 1, 2)$), and using (H3) we obtain

$$(k_{s1} + 6k_{s2})(\delta l_1 + \delta l_2 + \delta l_3) = \lambda/a_0. \quad \text{(E3)}$$

Substituting $\sum_{i=1}^{3}\delta l_i$ in (35) we take

$$\begin{aligned}
&(k_{s1} + 3k_{s2}/2)\,\delta l_{i'} + (\sqrt{3}/2)k_{s2}a_0(\delta\theta_{j'} - \delta\theta_{k'}) \\
&= (\lambda/a_0)\left[(2/3)\cos^2\theta_{0i'} - (3/2)k_{s2}/(k_{s1} + 6k_{s2})\right].
\end{aligned} \quad \text{(E4)}$$

Subtracting by parts equations (36) (two at a time) leads to

$$\begin{aligned}
&3\,(k_b' + k_{s2}/4)\,a_0^2(\delta\theta_{j'} - \delta\theta_{k'}) + \\
&(\sqrt{3}/4)a_0k_{s2}(3\delta l_{i'} - (\delta l_1 + \delta l_2 + \delta l_3)) \\
&= (\lambda/6)(\sin 2\theta_{0k'} - \sin 2\theta_{0j'}) \Longleftrightarrow \\
&(\sqrt{3}/4)a_0k_{s2}\delta l_{i'} + (k_b' + k_{s2}/4)\,a_0^2(\delta\theta_{j'} - \delta\theta_{k'}) \\
&= \frac{\lambda}{2\sqrt{3}}\left[\frac{2}{3}\cos^2\theta_{0i'} - \frac{1}{3} + \frac{k_{s2}}{2(k_{s1} + 6k_{s2})}\right].
\end{aligned} \quad \text{(E5)}$$

The solution of the system of (E4) and (E5) are (37) and (38).

Using the expressions of (37) and (38) for δl_i and $\delta\theta_j - \delta\theta_i$, and (H2), (H3), (H4), (H9) and (H11), (33) and (34) become

$$\begin{aligned}
\varepsilon &= \frac{2}{3a_0}\sum_{i=1}^{3}\cos^2\theta_{0i}3a_0(\xi_1'\cos^2\theta_{0i} + \xi_2') \\
&\quad -\frac{1}{3}\sum_{i=1}^{3}\sin 2\theta_{0i}\xi_3'(\sin 2\theta_{0j} - \sin 2\theta_{0i}) \\
&= 2\left[\xi_1'\sum_{i=1}^{3}\cos^4\theta_{0i} + \xi_2'\sum_{i=1}^{3}\cos^2\theta_{0i}\right] \\
&\quad -\frac{1}{3}\xi_3'\left[\sin 2\theta_{0j}\sum_{i=1}^{3}\sin 2\theta_{0i} - \sum_{i=1}^{3}\sin^2 2\theta_{0i}\right] \\
&= 2\left[\xi_1'(9/8) + \xi_2'(3/2)\right] - (1/3)\xi_3'\left[\sin 2\theta_{0j}\times 0 - (3/2)\right] \\
&= (9\xi_1' + 12\xi_2' + 2\xi_3')/4,
\end{aligned} \quad \text{(E6)}$$

and

$$\begin{aligned}
\delta\theta_i &= \frac{2}{3}\sum_{j=1}^{3}\cos^2\theta_{0j}\xi_3'(\sin 2\theta_{0j} - \sin 2\theta_{0i}) \\
&\quad -\sum_{j=1}^{3}\sin 2\theta_{0j}(\xi_1'\cos^2\theta_{0j} + \xi_2') \\
&= \frac{2\xi_3'}{3}\left[2\sum_{j=1}^{3}\cos^3\theta_{0j}\sin\theta_{0j} - \sin 2\theta_{0i}\sum_{j=1}^{3}\cos^2\theta_{0j}\right] \\
&\quad -2\xi_1'\sum_{j=1}^{3}\cos^3\theta_{0j}\sin\theta_{0j} - \xi_2'\sum_{j=1}^{3}\sin 2\theta_{0j} \\
&= (2\xi_3'/3)\left[2\times 0 - \sin 2\theta_{0i}\times(3/2)\right] - 2\xi_1'\times 0 - \xi_2'\times 0 \\
&= -\xi_3'\sin 2\theta_{0i},
\end{aligned} \quad \text{(E7)}$$

respectively, leading to (39).

Appendix F: Poisson's ratio

In order to find the Poisson's Ratio ν, ($\nu = -\varepsilon_\perp/\varepsilon$), we need to find the transverse strain $\varepsilon_\perp = \delta L_\perp/L_{\perp 0}$, where $L_{\perp 0}$ is a length of the material perpendicular to the strain direction and $\delta L_\perp$ its deformation upon tensile

strain ε. If $\mathbf{L}_{\perp 0} = t_a\mathbf{a} + t_b\mathbf{b}$ is a lattice vector, which is perpendicular to the vector $\mathbf{L}_0 = n\mathbf{a}+m\mathbf{b}$, which defines the strain direction, then

$$\begin{aligned}&\mathbf{L}_{\perp 0}\mathbf{L}_0 = 0 \Rightarrow (t_a\mathbf{a} + t_b\mathbf{b})(n\mathbf{a} + m\mathbf{b}) = 0 \Rightarrow\\ &t_a n(3a_0^2) + t_b m(3a_0^2) + (t_a m + t_b n)(3a_0^2)/2 = 0 \Rightarrow\\ &t_a(2n + m) + t_b(2m + n) = 0.\end{aligned} \tag{F1}$$

For convenience we may select t_a and t_b to be $t_a = 2m+n$ and $t_b = -(2n + m)$. Using (30), $\mathbf{L}_{\perp 0}$ becomes $\mathbf{L}_{\perp 0} = (m - n)\mathbf{r}_1 + (2n + m)\mathbf{r}_2 - (2m + n)\mathbf{r}_3$. The projection of the deformation of a bond vector normal to the strain direction is given by (10). Thus, the deformation $\delta L_\perp$ of $\mathbf{L}_{\perp 0}$ is

$$\delta L_\perp = \sum_{i=1}^{3} q_{\perp i}(\delta l_i \sin\theta_{0i} + a_0 \cos\theta_{0i}\delta\theta_i), \tag{F2}$$

where $q_{\perp 1} = m - n = 2L_0/(3a_0)(\cos\theta_{03} - \cos\theta_{02})$, $q_{\perp 2} = 2n + m = (n + m) + n = 2L_0/(3a_0)(\cos\theta_{01} - \cos\theta_{03})$ and $q_{\perp 3} = -(2m+n) = -m-(n+m) = 2L_0/(3a_0)(\cos\theta_{02} - \cos\theta_{01})$. Using (H14) we have

$$q_{\perp i} = 2L_0/(\sqrt{3}a_0)\sin\theta_{0i}, \tag{F3}$$

and consequently (using (42), (43), (49) and (H4))

$$\begin{aligned}\delta L_\perp &= \frac{2L_0}{\sqrt{3}a_0}\sum_{i=1}^{3}\sin\theta_{0i}(\delta l_i\sin\theta_{0i} + a_0\cos\theta_{0i}\delta\theta_i)\\ &= \frac{2L_0}{\sqrt{3}a_0}\sum_{i=1}^{3}\left[\sin^2\theta_{0i}3a_0(\xi_1\cos^2\theta_{0i} + \xi_2)\right.\\ &\quad \left. + a_0\sin\theta_{0i}\cos\theta_{0i}(-\xi_3\sin 2\theta_{0i})\right]\varepsilon\\ &= 2\sqrt{3}L_0\left[\frac{\xi_1}{4}\sum_{i=1}^{3}\sin^2 2\theta_{0i} + \xi_2\sum_{i=1}^{3}\sin^2\theta_{0i}\right.\\ &\quad \left. -\frac{\xi_3}{6}\sum_{i=1}^{3}\sin^2 2\theta_{0i}\right]\varepsilon\\ &= (3/2)2\sqrt{3}L_0\,(\xi_1/4 + \xi_2 - \xi_3/6)\,\varepsilon.\end{aligned} \tag{F4}$$

The magnitude $L_{\perp 0}$ of the vector $\mathbf{L}_{\perp 0}$ is

$$\begin{aligned}\mathrm{L}_{\perp 0} &= |(2m + n)\mathbf{a} - (2n + m)\mathbf{b}| = |-q_{\perp 3}\mathbf{a} - q_{\perp 2}\mathbf{b}|\\ &= 2L_0/(\sqrt{3}a_0)|\sin\theta_{02}\mathbf{a} + \sin\theta_{03}\mathbf{b}|\\ &= 2L_0(\sin^2\theta_{02} + \sin^2\theta_{03} + \sin\theta_{02}\sin\theta_{03})^{1/2}.\end{aligned}$$

Using (H2) and (H4)

$$\begin{aligned}&\sin^2\theta_{02} + \sin^2\theta_{03} + \sin\theta_{02}\sin\theta_{03}\\ &= (1/2)(\sin^2\theta_{02} + \sin^2\theta_{03}) +\\ &\quad (1/2)(\sin^2\theta_{02} + \sin^2\theta_{03} + 2\sin\theta_{02}\sin\theta_{03})\\ &= (1/2)(3/2 - \sin^2\theta_{01}) + (1/2)(\sin\theta_{02} + \sin\theta_{03})^2\\ &= 3/4 - (1/2)\sin^2\theta_{01} + (1/2)\sin^2\theta_{01} = 3/4.\end{aligned}$$

Thus,

$$L_{\perp 0} = 2L_0\sqrt{3/4} = \sqrt{3}L_0, \tag{F5}$$

and consequently,

$$\varepsilon_\perp = \delta L_\perp/L_{\perp 0} = (3\xi_1/4 + 3\xi_2 - \xi_3/2)\varepsilon, \tag{F6}$$

which leads to (55).

Appendix G: Derivation of Eqs. (57), (58), (59), (60)

The first of (57) can be directly obtained if we divide by parts (45) and (47). Using that equation, (46) becomes

$$\begin{aligned}\xi_2 &= k_{s1}k_{s2}(1 - 18k_b'/k_{s1})/K_0\\ &= k_{s1}k_{s2}(1 - (9/2)\xi_1/\xi_3)/K_0.\end{aligned} \tag{G1}$$

(47) can also be written as

$$\xi_3 = 2k_{s1}k_{s2}(6 + k_{s1}/k_{s2})/K_0 \tag{G2}$$

Dividing (G1) and (G2) by parts we obtain

$$\begin{aligned}&\xi_2/\xi_3 = [1 - (9/2)\xi_1/\xi_2]\,/\,[2(6 + k_{s1}/k_{s2})] \Rightarrow\\ &(6 + k_{s1}/k_{s2})\xi_2 = \xi_3/2 - 9\xi_1/4 \Rightarrow\\ &k_{s1}/k_{s2} = (2\xi_3 - 9\xi_1)/(4\xi_2) - 6 \Rightarrow\\ &k_{s2}/k_{s1} = 4\xi_2/(2\xi_3 - 9\xi_1 - 24\xi_2).\end{aligned} \tag{G3}$$

Using the first of (49), this equation leads to the second of (57).

From the expression $K_0 = k_{s1}^2 + 9k_{s1}k_{s2} + 18(k_{s1} + 3k_{s2})k_b'$, it is obvious that the expression $k_{s1}k_{s2}+2(2k_{s1}+3k_{s2})k_b'$, which appears in (53), is $k_{s1}k_{s2} + 2(2k_{s1} + 3k_{s2})k_b' = (K_0 - k_{s1}^2 + 18k_{s1}k_b')/9$. Thus, using (G1) and the second of (57),

$$\begin{aligned}&(k_{s1}k_{s2} + 2(2k_{s1} + 3k_{s2})k_b')/K_0\\ &= (1 - k_{s1}(k_{s1} - 18k_b')/K_0)/9 =\\ &= (1 - (k_{s1}/k_{s2})(k_{s2}(k_{s1} - 18k_b')/K_0))/9 =\\ &= (1 - \xi_2(k_{s1}/k_{s2}))/9\\ &= (1 + \xi_2(1 - \xi_3 + 3\xi_2)/\xi_2)/9\\ &= (2 - \xi_3 + 3\xi_2)/9.\end{aligned}$$

Thus,

$$\begin{aligned}A &= (k_{s1} + 6k_{s2})(2 - \xi_3 + 3\xi_2)/18\\ &= k_{s1}(1 + 6k_{s2}/k_{s1})(2 - \xi_3 + 3\xi_2)/18\\ &= k_{s1}[1 - 6\xi_2/(1 - \xi_3 + 3\xi_2)](2 - \xi_3 + 3\xi_2)/18\\ &= k_{s1}[(1 - \xi_3 - 3\xi_2)/(1 - \xi_3 + 3\xi_2)](2 - \xi_3 + 3\xi_2)/18.\end{aligned}$$

Using (49) (i.e. $2 - \xi_3 = 9\xi_1/2 + 6\xi_2$), we find

$$\begin{aligned}A &= k_{s1}\left(\frac{1 - \xi_3 - 3\xi_2}{1 - \xi_3 + 3\xi_2}\right)\frac{9\xi_1/2 + 6\xi_2 + 3\xi_2}{18}\\ &= k_{s1}\left(\frac{1 - \xi_3 - 3\xi_2}{1 - \xi_3 + 3\xi_2}\right)\frac{\xi_1 + 2\xi_2}{4}.\end{aligned} \tag{G4}$$

Solving this equation with respect to k_{s1} we get (58).

Using the expression in (58) for k_{s1} and (57), the derivation of (59) and (60) is obvious.

Appendix H: Useful relations between trigonometric functions of θ_{0i} of graphene

Some relations, which are used in the present study, between the trigonometric functions of the angles θ_{0i} defined by (32), are presented here.

As we have already seen in Sec. V B, $q_1 = -m$, $q_2 = -n$ and $q_3 = n+m$. Thus, $q_1+q_2+q_3 = 0$, and consequently, $\cos\theta_{01} + \cos\theta_{02} + \cos\theta_{03} = 0$, where $\theta_{0i} = \theta_{0i}(\theta_0) = 2\pi i/3 - \theta_0$, $i = 1, 2, 3$. Obviously, (i) $2\theta_{01}(\theta_0) = 4\pi/3 - 2\theta_0 = \theta_{02}(2\theta_0)$, $2\theta_{02}(\theta_0) = 8\pi/3 - 2\theta_0 = 2\pi + \theta_{01}(2\theta_0)$ and $2\theta_{03}(\theta_0) = 4\pi - 2\theta_0 = 2\pi + \theta_{03}(2\theta_0)$, and (ii) $4\theta_{01}(\theta_0) = 8\pi/3 - 4\theta_0 = 2\pi + \theta_{01}(4\theta_0)$, $4\theta_{02}(\theta_0) = 16\pi/3 - 2\theta_0 = 4\pi + \theta_{02}(4\theta_0)$ and $4\theta_{03}(\theta_0) = 8\pi - 2\theta_0 = 6\pi + \theta_{03}(4\theta_0)$. Consequently, for $k = 1$, or 2, or 4,

$$\cos(k\theta_{01}) + \cos(k\theta_{02}) + \cos(k\theta_{03}) = 0. \tag{H1}$$

The first derivative of the above equation with respect to θ_0 gives

$$\sin(k\theta_{01}) + \sin(k\theta_{02}) + \sin(k\theta_{03}) = 0. \tag{H2}$$

Using (H1) for $k = 2$ or $k = 4$, and the relation $\cos 2\theta = 2\cos^2\theta - 1$ we obtain

$$\begin{aligned}\cos^2(2\theta_{01}) + \cos^2(2\theta_{02}) + \cos^2(2\theta_{03}) \ &= \\ \cos^2\theta_{01} + \cos^2\theta_{02} + \cos^2\theta_{03} \ &= \ 3/2.\end{aligned} \tag{H3}$$

Then, using the relation $\sin^2\theta = 1 - \cos^2\theta$, we obtain

$$\begin{aligned}\sin^2(2\theta_{01}) + \sin^2(2\theta_{02}) + \sin^2(2\theta_{03}) \ &= \\ \sin^2\theta_{01} + \sin^2\theta_{02} + \sin^2\theta_{03} \ &= \ 3/2.\end{aligned} \tag{H4}$$

Moreover, using the relation $\sin 2\theta = 2\sin\theta\cos\theta$, (H2) for $k = 2$ yields

$$\sin\theta_{01}\cos\theta_{01} + \sin\theta_{02}\cos\theta_{02} + \sin\theta_{03}\cos\theta_{03} = 0. \tag{H5}$$

Using (H1) for $k = 1$ and (H3), we obtain

$$\begin{aligned}&(\cos\theta_{01} + \cos\theta_{02} + \cos\theta_{03})^2 = 0 \Rightarrow \\ &\cos^2\theta_{01} + \cos^2\theta_{02} + \cos^2\theta_{03} + 2\cos\theta_{01}\cos\theta_{02} + \\ &\qquad 2\cos\theta_{02}\cos\theta_{03} + 2\cos\theta_{03}\cos\theta_{01} = 0 \Rightarrow \\ &\cos\theta_{01}\cos\theta_{02} + \cos\theta_{02}\cos\theta_{03} \\ &\qquad + \cos\theta_{03}\cos\theta_{01} = -3/4.\end{aligned} \tag{H6}$$

In turn, using (H2) for $k = 1$ and (H4), we obtain

$$\sin\theta_{01}\sin\theta_{02} + \sin\theta_{02}\sin\theta_{03} + \sin\theta_{03}\sin\theta_{01} = -\frac{3}{4}. \tag{H7}$$

Thus,

$$\begin{aligned}&(\cos\theta_{01}\cos\theta_{02} + \cos\theta_{02}\cos\theta_{03} + \\ &\qquad \cos\theta_{03}\cos\theta_{01})^2 = 9/16 \Rightarrow \\ &\cos^2\theta_{01}\cos^2\theta_{02} + \cos^2\theta_{02}\cos^2\theta_{03} + \cos^2\theta_{03}\cos^2\theta_{01} + \\ &2\cos\theta_{01}\cos\theta_{02}\cos\theta_{03}(\cos\theta_{01} + \cos\theta_{02} + \\ &\qquad \cos\theta_{03}) = 9/16 \Rightarrow \\ &\cos^2\theta_{01}\cos^2\theta_{02} + \cos^2\theta_{02}\cos^2\theta_{03} + \\ &\qquad \cos^2\theta_{03}\cos^2\theta_{01} = 9/16.\end{aligned} \tag{H8}$$

Consequently, (H3) gives

$$\begin{aligned}&(\cos^2\theta_{01} + \cos^2\theta_{02} + \cos^2\theta_{03})^2 = 9/4 \Rightarrow \\ &\cos^4\theta_{01} + \cos^4\theta_{02} + \cos^4\theta_{03} + 2(\cos^2\theta_{01}\cos^2\theta_{02} + \\ &\cos^2\theta_{02}\cos^2\theta_{03} + \cos^2\theta_{03}\cos^2\theta_{01}) = 9/4 \Rightarrow \\ &\cos^4\theta_{01} + \cos^4\theta_{02} + \cos^4\theta_{03} = 9/8,\end{aligned} \tag{H9}$$

and in turn, (H4) gives

$$\begin{aligned}&(\sin^2\theta_{01} + \sin^2\theta_{02} + \sin^2\theta_{03})^2 = 9/4 \Rightarrow \\ &\sin^4\theta_{01} + \sin^4\theta_{02} + \sin^4\theta_{03} + 2(\sin^2\theta_{01}\sin^2\theta_{02} + \\ &\sin^2\theta_{02}\sin^2\theta_{03} + \sin^2\theta_{03}\sin^2\theta_{01}) = 9/4 \Rightarrow \\ &\sin^4\theta_{01} + \sin^4\theta_{02} + \sin^4\theta_{03} = 9/8.\end{aligned} \tag{H10}$$

Taking the first derivative of (H9), we obtain

$$\sum_{i=1}^{3}\cos^3\theta_{0i}\sin\theta_{0i} = 0. \tag{H11}$$

Moreover, let us consider the trigonometric identity

$$\begin{aligned}&\sin(m\theta_{0j}) - \sin(m\theta_{0i}) = \\ &\qquad = 2\sin[m(\theta_{0j} - \theta_{0i})/2]\cos[m(\theta_{0i} + \theta_{0j})/2].\end{aligned}$$

For the angles θ_{0i} in (32) we have $(\theta_{0j} - \theta_{0i})/2 = (j - i)\pi/3$ and $(\theta_{0j} + \theta_{0i})/2 = (i + j)\pi/3 - \theta_0$. For $(i, j, k) = (1, 2, 3)$, or $(2, 3, 1)$, or $(3, 1, 2)$, the sum $i + j + k = 6$, and consequently, $i + j = 6 - k$. Thus, $(i + j)\pi/3 - \theta_0 = (6 - k)\pi/3 - \theta_0 = 2\pi - k\pi/3 - \theta_0 = 2\pi - k\pi + \theta_{0k}$. Consequently, $\cos[m(\theta_{0i} + \theta_{0j})/2] = \cos[m(\theta_{0k} - k\pi)]$ and $\sin[m(\theta_{0j} - \theta_{0i})/2] = \sin[m(j - i)\pi/3]$. Thus, for $m = 1$

$$\sin\theta_{0j'} - \sin\theta_{0i'} = -\sqrt{3}\cos\theta_{0k'}, \tag{H12}$$

and for $m = 2$

$$\sin 2\theta_{0j'} - \sin 2\theta_{0i'} = \sqrt{3}\cos 2\theta_{0k'}. \tag{H13}$$

Taking the first derivative of (H12) with respect to θ_0 we obtain

$$\cos\theta_{0j'} - \cos\theta_{0i'} = \sqrt{3}\sin\theta_{0k'}. \tag{H14}$$

[1] Bolotin K, Sikes K, Jiang Z, Klima M, Fudenberg G, Hone J, Kim P and Stormer H 2008 *Solid State Commun.* **146** 351 – 355

[2] Fthenakis Z G and Tománek D 2012 *Phys. Rev. B* **86**(12) 125418

[3] Ghosh S, Calizo I, Teweldebrhan D, Pokatilov E P, Nika D L, Balandin A A, Bao W, Miao F and Lau C N 2008 *Appl. Phys. Lett.* **92** 151911

[4] Cai W, Moore A L, Zhu Y, Li X, Chen S, Shi L and Ruoff R S 2010 *Nano Lett.* **10** 1645–1651

[5] Fthenakis Z G and Lathiotakis N N 2015 *Phys. Chem. Chem. Phys.* **17**(25) 16418–16427

[6] Lee C, Wei X, Kysar J W and Hone J 2008 *Science* **321** 385–388

[7] Castellanos-Gomez A, Singh V, van der Zant H S J and Steele G A 2015 *Ann. Physik* **527** 27–44

[8] Peng Q, Ji W and De S 2012 *Comput. Mater. Sci.* **56** 11 – 17

[9] Kudin K N, Scuseria G E and Yakobson B I 2001 *Phys. Rev. B* **64**(23) 235406

[10] Li T 2012 *Phys. Rev. B* **85**(23) 235407

[11] Zhao H 2012 *Phys. Lett. A* **376** 3546 – 3550

[12] Peng Q, Wen X and De S 2013 *RSC Adv.* **3**(33) 13772–13781

[13] Wei Q and Peng X 2014 *Appl. Phys. Lett.* **104** 251915

[14] Fthenakis Z G and Menon M 2017 *to be published*

[15] Tang Q, Zhou Z and Chen Z 2015 *Wiley Interdiscipl. Rev.: Comput. Mol. Sci.* **5** 360–379

[16] Bhimanapati G R, Lin Z, Meunier V, Jung Y, Cha J, Das S, Xiao D, Son Y, Strano M S, Cooper V R, Liang L, Louie S G, Ringe E, Zhou W, Kim S S, Naik R R, Sumpter B G, Terrones H, Xia F, Wang Y, Zhu J, Akinwande D, Alem N, Schuller J A, Schaak R E, Terrones M and Robinson J A 2015 *ACS Nano* **9** 11509–11539

[17] Chhowalla M, Liu Z and Zhang H 2015 *Chem. Soc. Rev.* **44**(9) 2584–2586

[18] Ooi N, Rairkar A, Lindsley L and Adams J B 2006 *J. Phys.: Cond. Matter* **18** 97

[19] Le M Q 2014 *J. Comp. Theor. Nanosci.* **11** 1458–1464

[20] Andriotis A N, Richter E and Menon M 2016 *Phys. Rev. B* **93**(8) 081413

[21] Hansson A, de Brito Mota F and Rivelino R 2012 *Phys. Rev. B* **86**(19) 195416

[22] Dai J, Zhao Y, Wu X, Yang J and Zeng X C 2013 *J. Phys. Chem. Lett.* **4** 561–567

[23] Tan X, Li F and Chen Z 2014 *J. Phys. Chem. C* **118** 25825–25835

[24] Ding Y and Wang Y 2013 *J. Phys. Chem. C* **117** 18266–18278

[25] Garg P, Kumar S, Choudhuri I, Mahata A and Pathak B 2016 *J. Phys. Chem. C* **120** 7052–7060

[26] Tsipas P, Kassavetis S, Tsoutsou D, Xenogiannopoulou E, Golias E, Giamini S A, Grazianetti C, Chiappe D, Molle A, Fanciulli M and Dimoulas A 2013 *Appl. Phys. Lett.* **103** 251605

[27] Bacaksiz C, Sahin H, Ozaydin H D, Horzum S, Senger R T and Peeters F M 2015 *Phys. Rev. B* **91**(8) 085430

[28] Peng Q, Chen X J, Liu S and De S 2013 *RSC Adv.* **3**(19) 7083–7092

[29] Qin R, Wang C H, Zhu W and Zhang Y 2012 *AIP Advances* **2** 022159

[30] Kaloni T P, Schreckenbach G, Freund M S and Schwingenschlögl U 2016 *phys. stat. sol. (RRL)* **10** 133–142

[31] Jamdagni P, Kumar A, Thakur A, Pandey R and Ahluwalia P K 2015 *Mater. Res. Express* **2** 016301

[32] Liu H, Neal A T, Zhu Z, Luo Z, Xu X, Tománek D and Ye P D 2014 *ACS Nano* **8** 4033–4041

[33] Enyashin A N and Ivanovskii A L 2011 *phys. stat. sol. (b)* **248** 1879–1883

[34] Zhang S, Zhou J, Wang Q, Chen X, Kawazoe Y and Jena P 2015 *Proc. Nat. Acad. Sci.* **112** 2372–2377

[35] Peng Q, Dearden A K, Crean J, Han L, Liu S, Wen X and De S 2014 *Nanotech. Sci. Appl.* **7** 1–29

[36] Pumera M and Wong C H A 2013 *Chem. Soc. Rev.* **42**(14) 5987–5995

[37] Zhu Z, Fthenakis Z G and Tománek D 2015 *2D Materials* **2** 035001

[38] Sun Y and Liew K 2010 Multiscale modeling of carbon nanotubes *Trends in Computational Nanomechanics* (*Challenges and Advances in Computational Chemistry and Physics* vol 9) ed Dumitrica T (Springer Netherlands) pp 367–388

[39] Geng J and Chang T 2006 *Phys. Rev. B* **74**(24) 245428

[40] Chang T and Gao H 2003 *J. Mech. Phys. Solids* **51** 1059 – 1074

[41] Zhao J, Wang L, Jiang J W, Wang Z, Guo W and Rabczuk T 2013 *J. Appl. Phys.* **113** 063509

[42] Zhao J, Lu L and Rabczuk T 2014 *J. Chem. Phys.* **140** 204704

[43] Zhao J, Jiang J W, Wang L, Guo W and Rabczuk T 2014 *J. Mech. Phys. Solids* **71** 197 – 218

[44] Jiang L and Guo W 2011 *J. Mech. Phys. Solids* **59** 1204 – 1213

[45] Davydov S Y 2010 *Phys. Solid State* **52** 810–812

[46] Kalosakas G, Lathiotakis N N, Galiotis C and Papagelis K 2013 *J. Appl. Phys.* **113** 134307

[47] Lobo C and Martins L J 1997 *Z. Phys. D* **39** 159–164

[48] Giannozzi P, Baroni S, Bonini N, Calandra M, Car R, Cavazzoni C, Ceresoli D, Chiarotti G L, Cococcioni M, Dabo I, Dal Corso A, de Gironcoli S, Fabris S, Fratesi G, Gebauer R, Gerstmann U, Gougoussis C, Kokalj A, Lazzeri M, Martin-Samos L, Marzari N, Mauri F, Mazzarello R, Paolini S, Pasquarello A, Paulatto L, Sbraccia C, Scandolo S, Sclauzero G, Seitsonen A P, Smogunov A, Umari P and Wentzcovitch R M 2009 *J. Phys.: Cond. Matter* **21** 395502 (19pp)

[49] Perdew J P, Burke K and Ernzerhof M 1996 *Phys. Rev. Lett.* **77** 3865

[50] Rappe A M, Rabe K, Kaxiras E and Joannopoulos J 1990 *Phys. Rev. B* **41** R1227

[51] Dal Corso A C.pbe-rrkjus.upf `http://www.quantum-espresso.org/wp-content/uploads/\upf_file`